

Studies of light exotic nuclei with radioactive beams at FLNR, JINR

E. Yu. Nikolskii ^{1,2} (on behalf of ACCULINNA group)

¹ Joint Institute for Nuclear Research, Flerov Laboratory of Nuclear Reactions



² National Research Center “Kurchatov Institute”



COLLABORATION:

National Research Nuclear University “MEPhI”, 115409 Moscow, Russia

Dubna State University, 141982 Dubna, Russia

Heavy Ion Laboratory, University of Warsaw, 02-093 Warsaw, Poland

Skobeltsyn Institute of Nuclear Physics, Moscow State University, 119991 Moscow, Russia

GSI Helmholtzzentrum für Schwerionenforschung GmbH, 64291 Darmstadt, Germany

II. Physikalisches Institut, Justus-Liebig-Universität, 35392 Giessen, Germany

Laboratory of Information Technologies, JINR, 141980 Dubna, Russia

Institute of Nuclear Physics, 050032 Almaty, Kazakhstan

Nuclear Research Institute, 670000 Dalat, Vietnam

Bogoliubov Laboratory of Theoretical Physics, JINR, 141980 Dubna, Russia

AGH University of Science and Technology, Faculty of Physics and Applied Computer Science, 30-059 Krakow, Poland

Institute of Nuclear Physics PAN, Radzikowskiego 152, 31342 Kraków, Poland

Department of Physics, Chalmers University of Technology, S-41296 Göteborg, Sweden

Seoul, April 2019



Korea University – JINR MOU Ceremony 2019



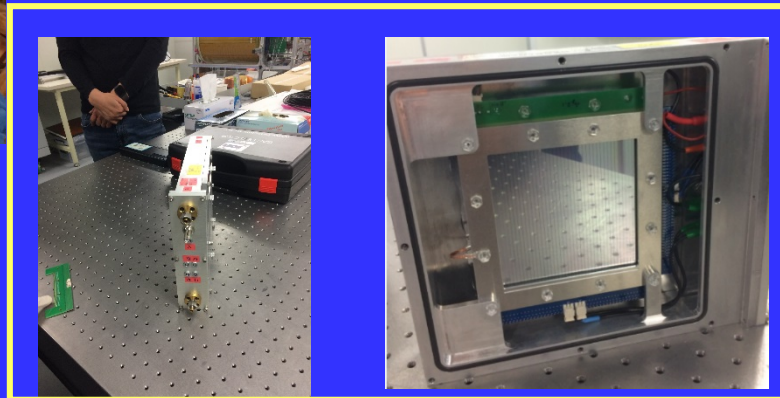
Meat restaurant in Daejeon. Delicious!!!



RAON, April 2019



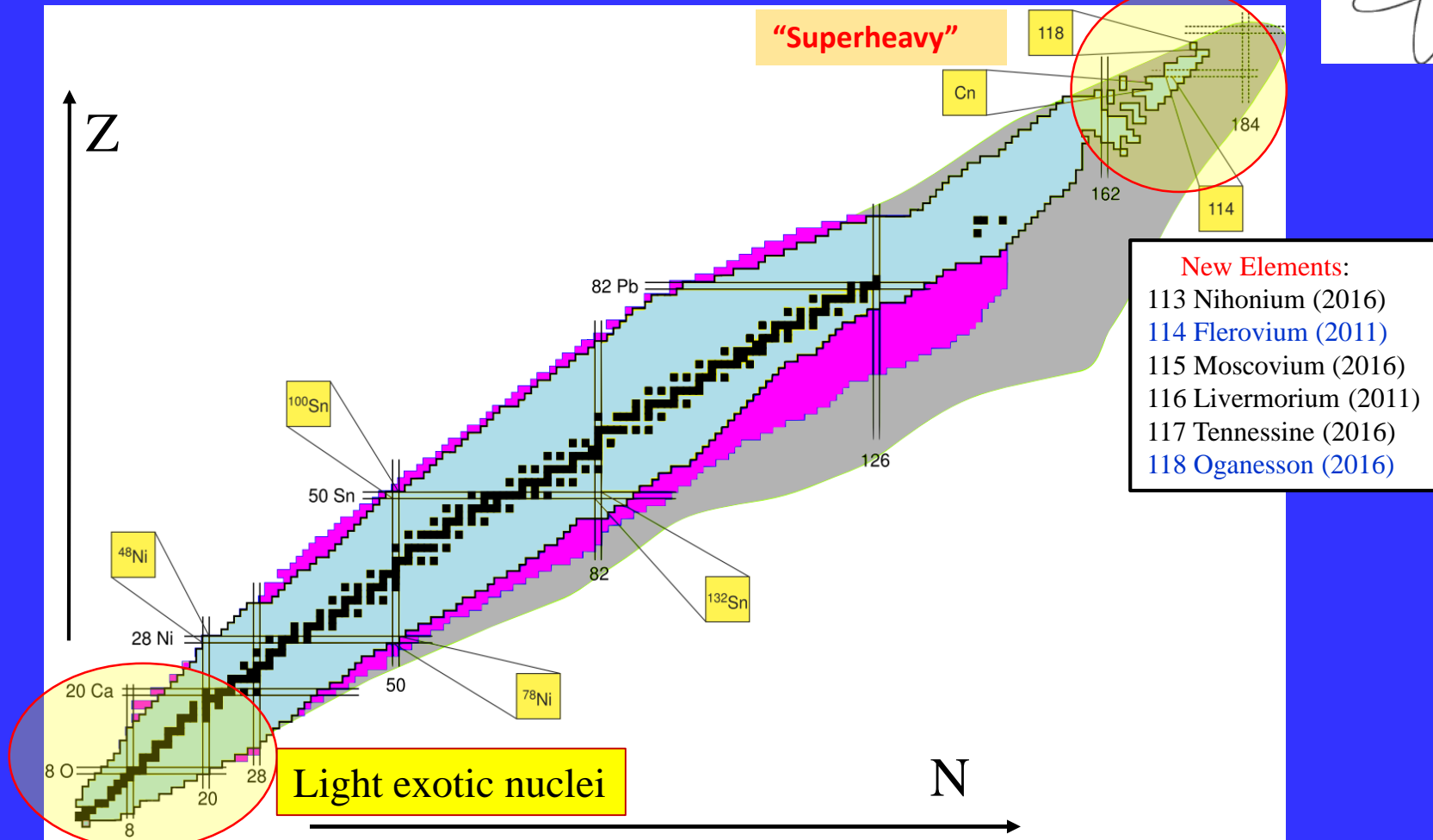
Detector PPAC, 3 of them are in Dubna now



OUTLINE:

- Physics motivation. Light exotic nuclei near and beyond nucleon drip lines
- Dubna accelerator complex at Flerov Laboratory of Nuclear Reactions, JINR
 - ACCULINNA fragment separator layout
 - Gaseous cryogenic targets, including unique tritium target
- Short overview of experiments at ACCULINNA fragment separator
 - Elastic scattering (${}^6\text{He}+{}^4\text{He}$). Looking on $2n$ -transfer
 - Study of ${}^6\text{He}$ nucleus structure by QFS reaction ${}^4\text{He}({}^6\text{He},\alpha\alpha)2n$
 - Search for ${}^5\text{H}$ resonances by $p({}^6\text{He},pp){}^5\text{H}$, $d({}^6\text{He},{}^3\text{He}){}^5\text{H}$ and $t(t,p){}^5\text{H}$ reactions
 - Correlation measurements to study ${}^9\text{He}$ and ${}^{10}\text{He}$ systems with ${}^8\text{He}$ beam
- New fragment separator ACCULINNA-2 at FLNR, JINR. Experimental setup.
 - Calibration reactions ${}^2\text{H}({}^{10}\text{Be},{}^3\text{He}){}^9\text{Li}$ and ${}^2\text{H}({}^{10}\text{Be},{}^4\text{He}){}^8\text{Li}$ with ${}^{10}\text{Be}$ beam
 - Study of the ${}^7\text{H}$ system via ${}^2\text{H}({}^8\text{He},{}^3\text{He}){}^7\text{H} \rightarrow t + 4n$. Two Runs
 - Satellite study of the ${}^6\text{H}$ system in the reaction ${}^2\text{H}({}^8\text{He},{}^4\text{He}){}^6\text{H} \rightarrow t + 3n$
- Looking ahead
- Summary

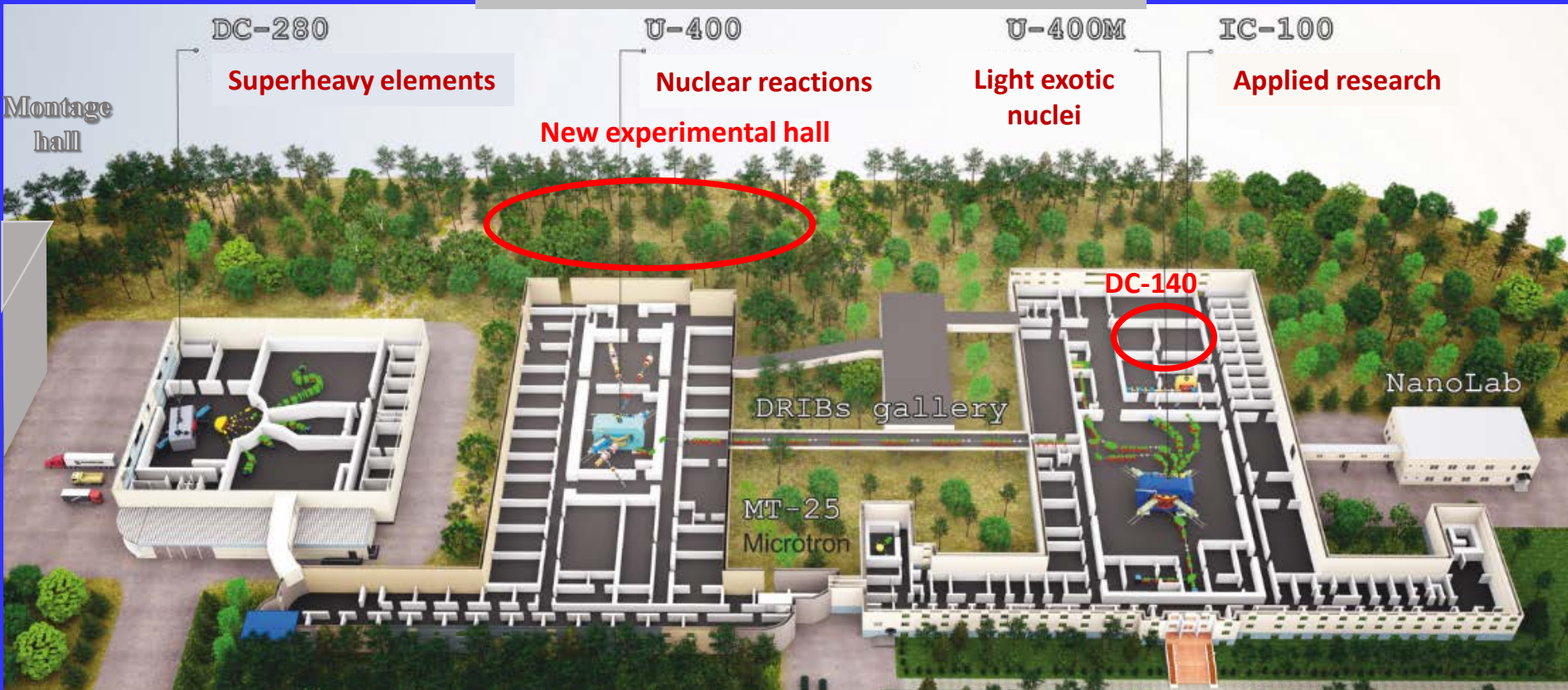
Main areas of interest at FLNR, JINR



$4,5\text{H}, 6\text{H}, 7\text{H}, 7\text{He}, 6,8,9,10\text{He}, 10\text{Li}, 6\text{Be}, 17\text{Ne}, 27\text{S}$

DUBNA ACCELERATOR COMPLEX

FLEROV LABORATORY OF NUCLEAR REACTIONS



Setups:
DGFRS-2
GRAND

DC-280



Setups:
SHELS
MAVR
CORSET

U-400



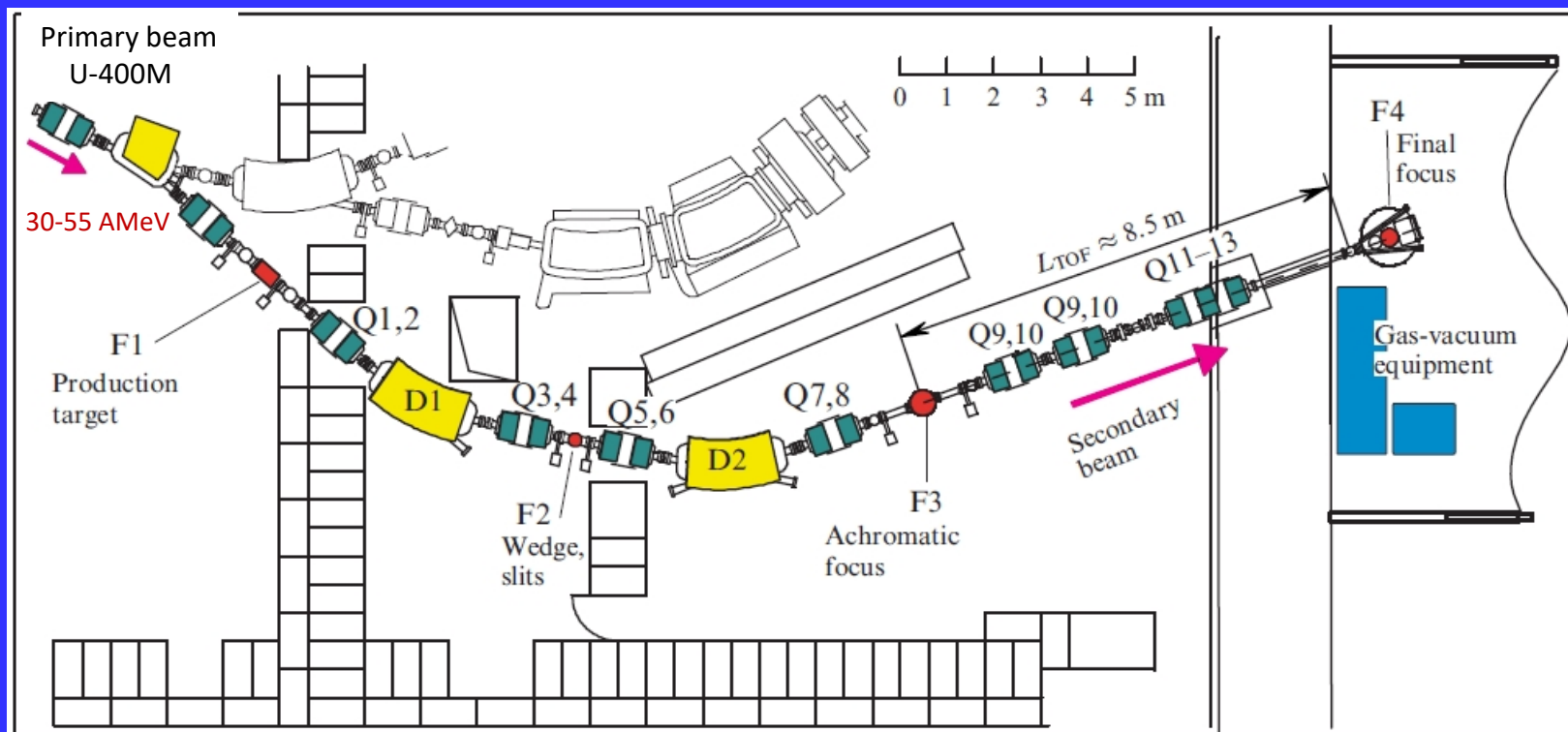
Setups:
ACCULINNA-2
COMBAS
MASHA

U-400M (modernization)

ACCULINNA fragment separator (since 1996)

<http://aculina.jinr.ru/>

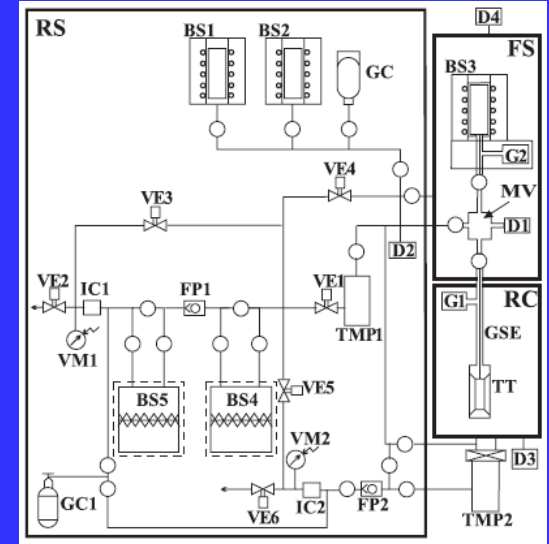
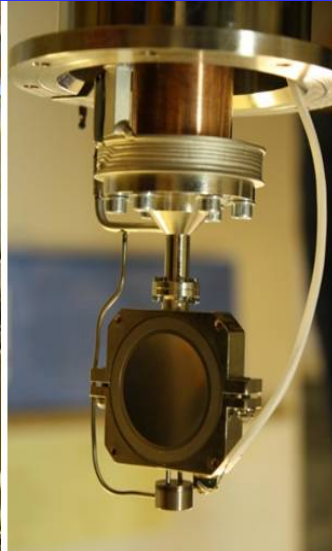
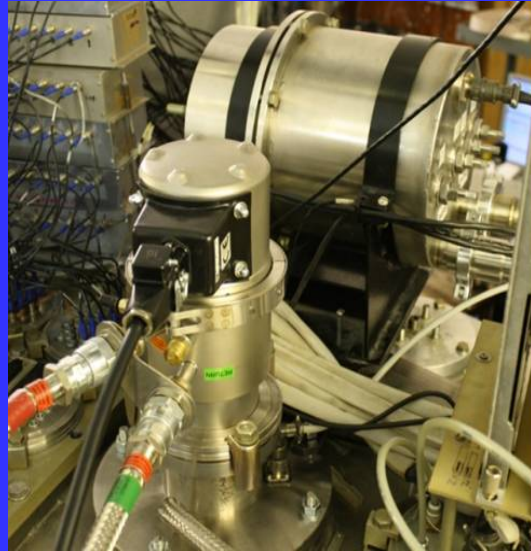
[Rodin A.M. et al. Nucl. Instrum. Meth. Phys. Res. B **204** 114 (2003)]



${}^6\text{He}$ ($\sim 10^6 \text{ s}^{-1}$) and ${}^8\text{He}$ ($\sim 10^4 \text{ s}^{-1}$) secondary beams at $\sim 25 \text{ A MeV}$
 ${}^3\text{H}$ beam ($3 \times 10^7 \text{ s}^{-1}$) at 58 MeV

- Elastic scattering (${}^6\text{He}+{}^4\text{He}$) & (${}^8\text{He}+{}^4\text{He}$). Looking on $2n$ & $4n$ transfers at backward angles
- Study of ${}^6\text{He}$ nucleus structure by QFS reaction on ${}^4\text{He}$ target
- Search for ${}^5\text{H}$ resonances by $p({}^6\text{He}, pp){}^5\text{H}$, $d({}^6\text{He}, {}^3\text{He}){}^5\text{H}$ and $t(t, p){}^5\text{H}$ reactions
- Correlation measurements to study ${}^9\text{He}$ and ${}^{10}\text{He}$ systems with ${}^8\text{He}$ beam

Unique tritium (^3H) gas/liquid target at ACCULINNA



A.A. Yukhimchuk et al.,
NIM A 513 (2003) 439

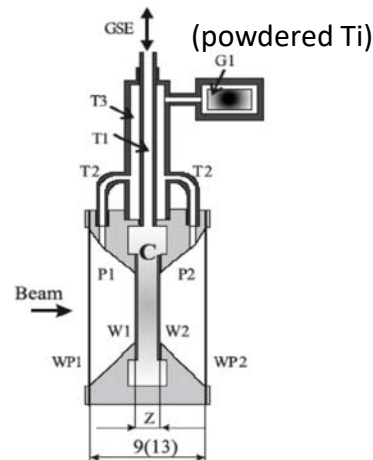
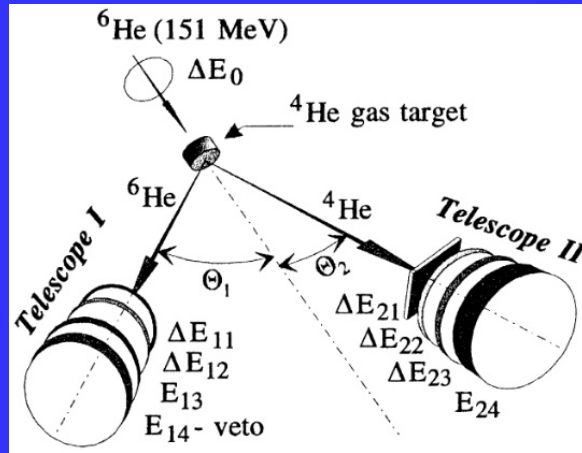


Fig. 2. Schematic drawing of the target. Denoted in the drawing are: C—target cell; W1, W2—cell windows; GSE (tube T1)—gas supply/evacuation path; P1, P2—protection barriers supplied with windows (WP1, WP2) and connected with the getter G1 through the tubes T1, T2 and T3.

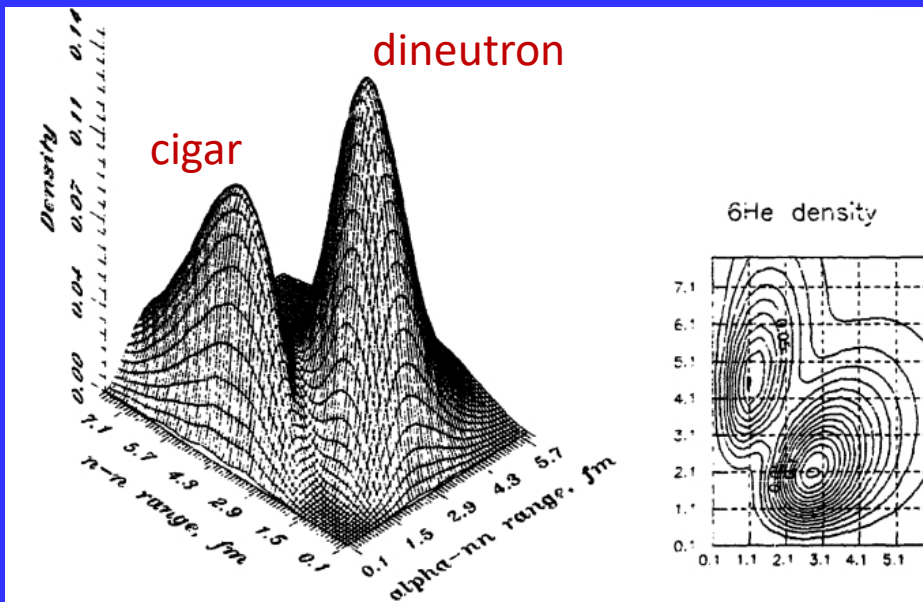
Gas:
 $\phi=25$ mm, $d=3\div 6$ mm,
 $T=26$ K, $P=0.92$ atm,
 $3\cdot 10^{20}$ Atoms/cm 2

Liquid:
 $\phi=20$ mm, $d=0.4\div 0.8$ mm,
 $w=2\times 8.4$ μ stainless steel,
 $1.1\cdot 10^{21}$ Atoms/cm 2
 $I \leq 960$ Ci ($3.54\cdot 10^{13}$ Bq)

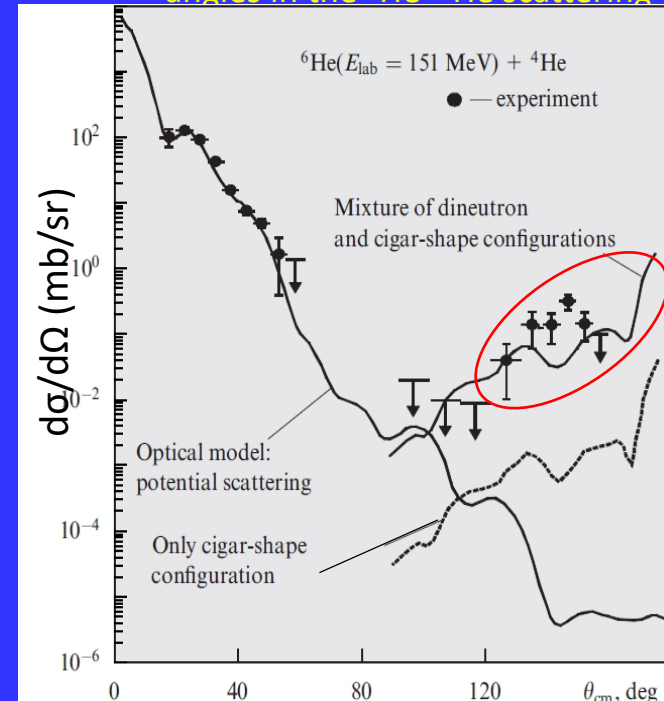
Dineutron structure of the ${}^6\text{He}$ nucleus with neutron halo in the ${}^6\text{He}+{}^4\text{He}$ elastic scattering



Spatial structure of ${}^6\text{He}$ nucleus (HH-theoretical calculations)

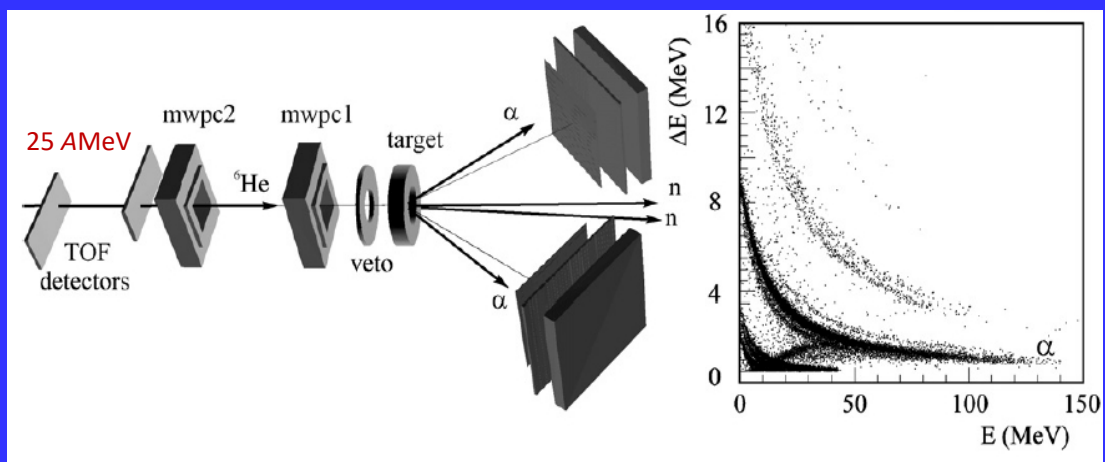


Clear signal of two neutrons exchange at backward angles in the ${}^6\text{He}+{}^4\text{He}$ scattering

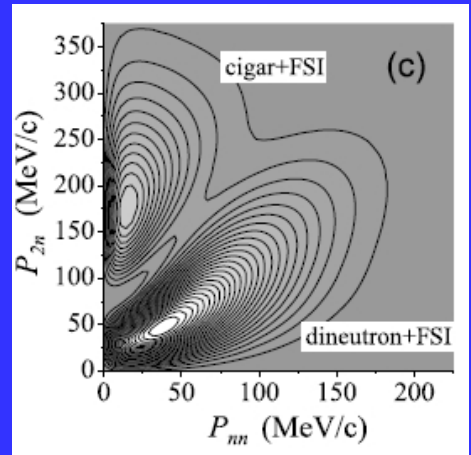


G.M. Ter-Akopian et al., PLB 426 (1998) 251–256

Study of the ${}^6\text{He}$ structure in the reaction of **quasifree** scattering ${}^4\text{He}({}^6\text{He}, 2\alpha)$

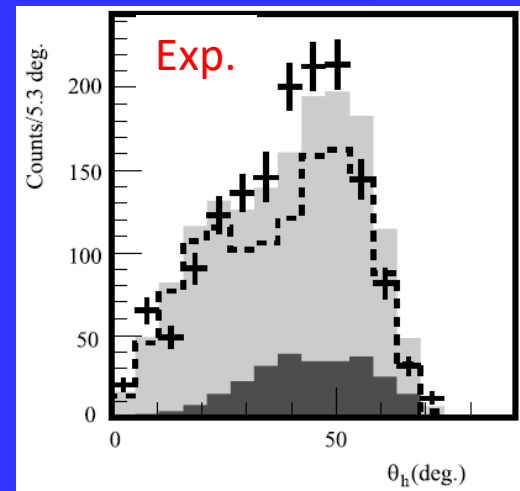
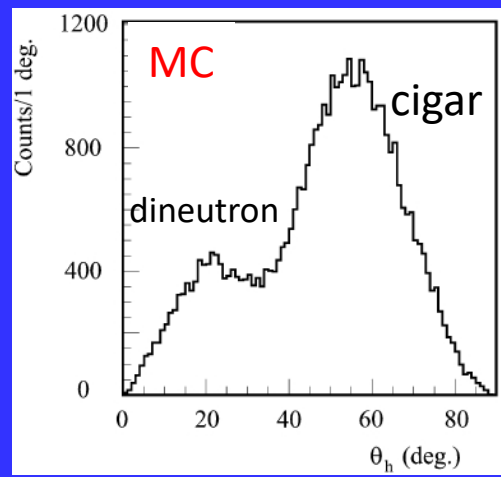
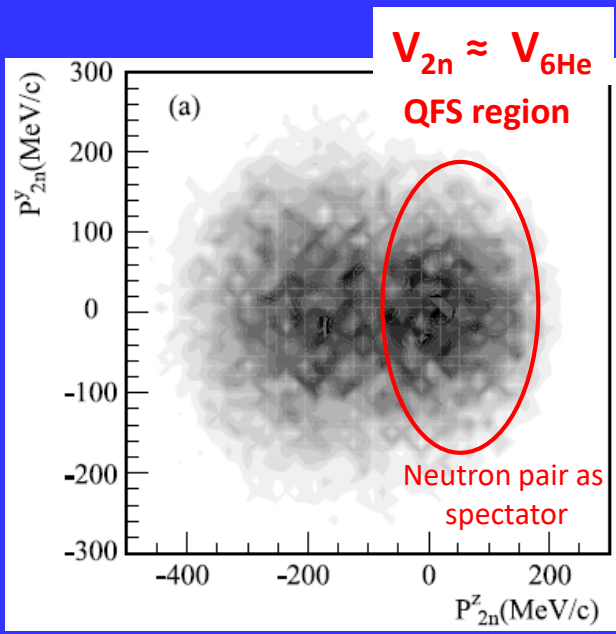


Spectral function ${}^6\text{He} |S(P_{nn}, P_{2n})|^2$



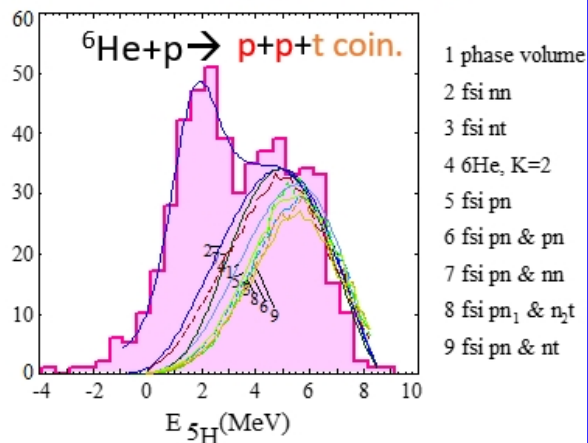
Hyper-angle:

$$\tan \theta_x = \sqrt{\frac{E_{nn}}{E_{\alpha-2n}}}$$



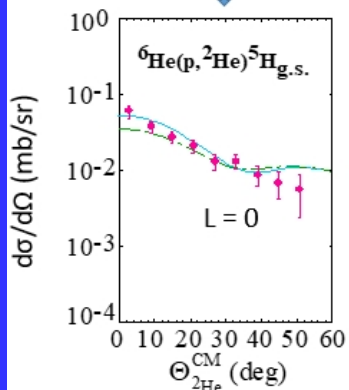
S.I. Sidorchuk et al., Nucl. Phys. A840 (2010) 1

^5H : $E_{\text{obs}} = 1.7 \pm 0.3 \text{ MeV}$
 $\Gamma_{\text{obs}} = 1.9 \pm 0.4 \text{ MeV}$



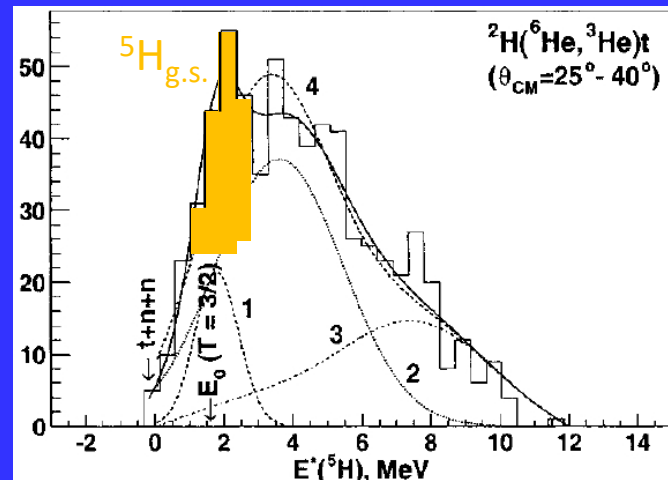
Collaboration: Dubna-Kurchatov-RIKEN-GANIL

Indication for $^5\text{H}_{\text{g.s.}} (1/2^+)$



$^2\text{H}(^6\text{He}, ^3\text{He})^5\text{H}$

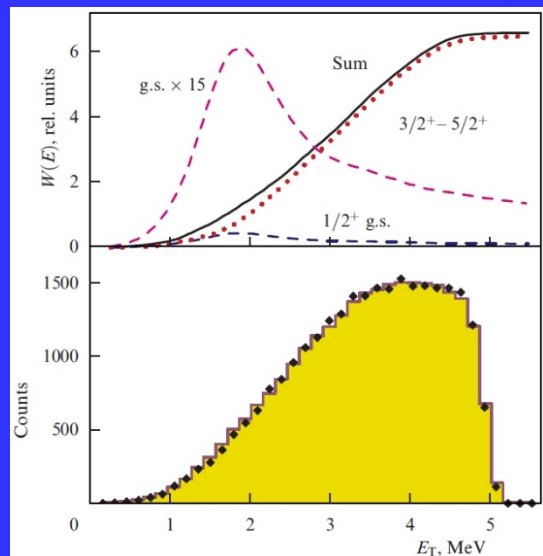
S.V. Stepanyov et al., Nucl. Phys. A738 (2004) 436



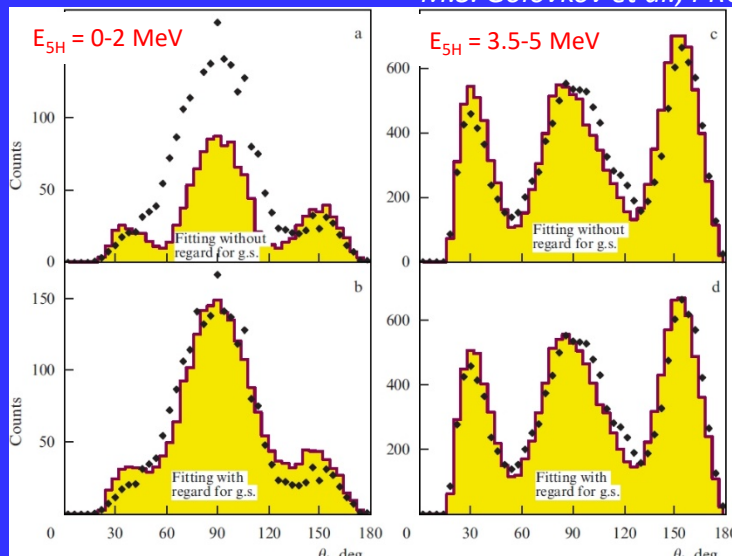
$^3\text{H}(^3\text{H}, p)^5\text{H}$ (p-t-n coincidences, complete kinematics)

M.S. Golovkov et al., PRL 93, 262501 (2004)

M.S. Golovkov et al., PRC 72, 064612 (2005)



Target: T_2 gas 4 mm, 25K, 0.86 atm
 Beam 58 MeV, $3 \times 10^7 \text{ s}^{-1}$



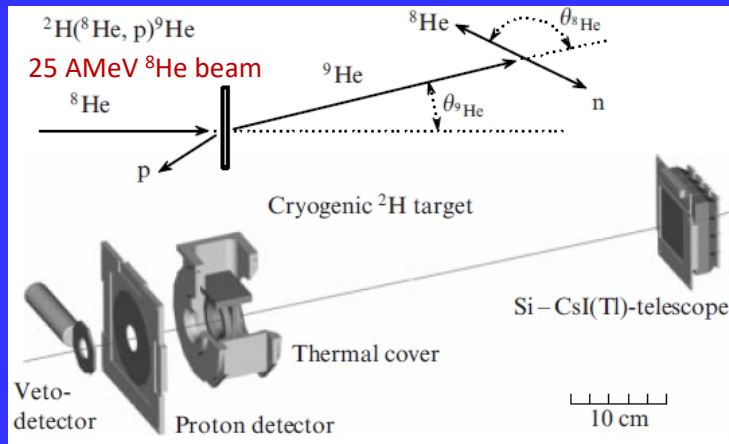
interference of $1/2^+, 3/2^+$
 and $5/2^+$ states

interference of only
 $3/2^+$ and $5/2^+$ states

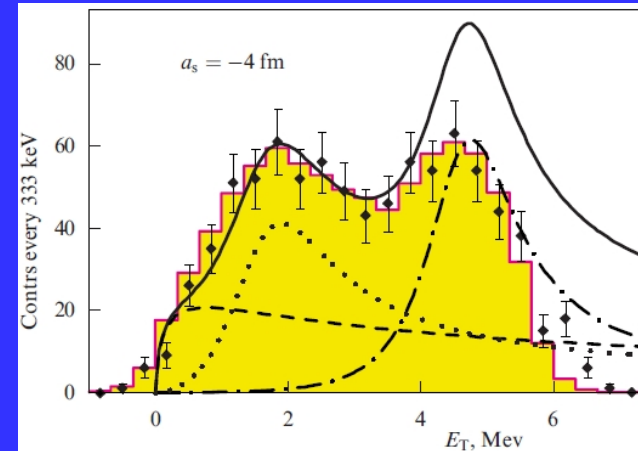
$E_{\text{g.s.}} \approx 1.8 \text{ MeV}$
 $\Gamma \approx 1.3 \text{ MeV}$

Unambiguous spectrum identification of ${}^9\text{He}$ in the $d({}^8\text{He}, p){}^9\text{He}$ reaction

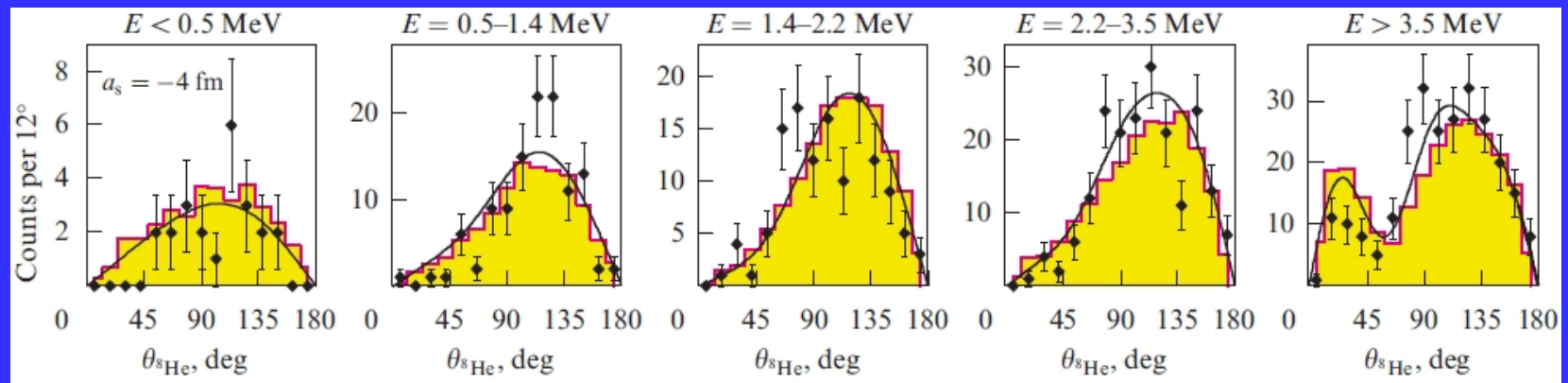
M.S. Golovkov et al., PRC 76, 021605(R) (2007)



Setup: complete kinematics



${}^9\text{He}$ missing mass spectrum

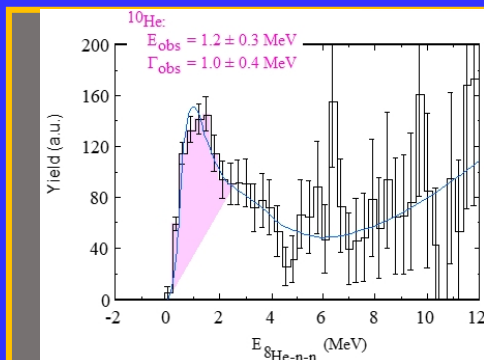


Angular distributions of ${}^8\text{He}$ in CM of ${}^9\text{He}$

Conclusions: the lowest resonant state of ${}^9\text{He}$ is found at 2.0 ± 0.2 MeV with a width of ~ 2 MeV and is identified as $1/2^-$. Angular correlations are uniquely explained by the interference of the $1/2^-$ resonance with a virtual $1/2^+$ state (a limit $a > -20$ fm is obtained for the scattering length), and with a $5/2^+$ resonance at energy ≥ 4.2 MeV.

Structure of ^{10}He low-lying states uncovered by correlations

S.I. Sidorchuk et al., PRL 108, 202502 (2012)

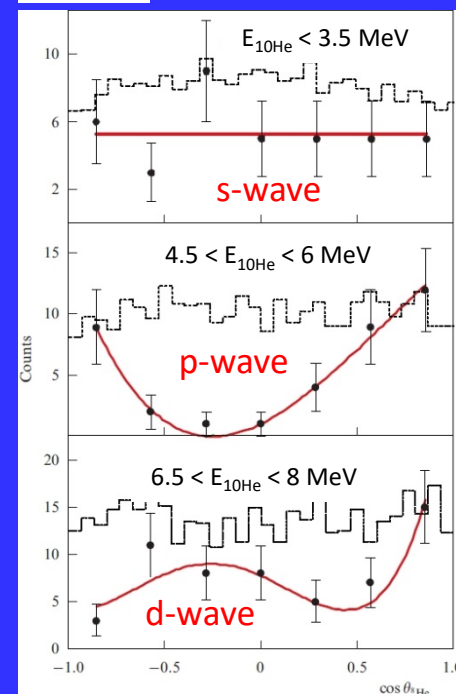


First observation of ^{10}He (RIKEN)
A. A. Korshennikov et al., PLB 326 (1994) 31

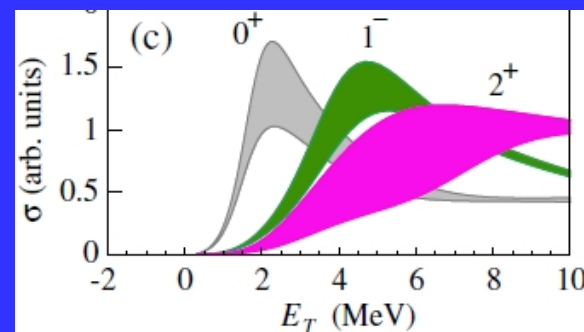
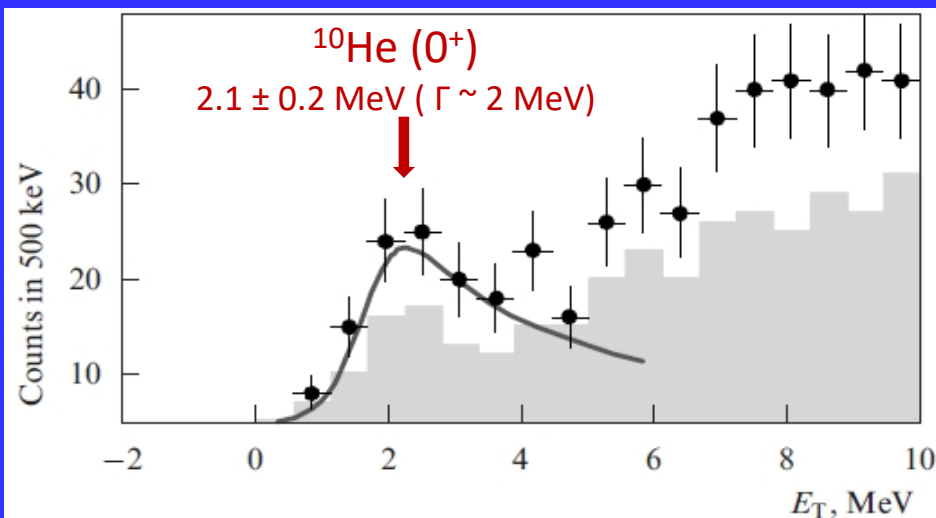
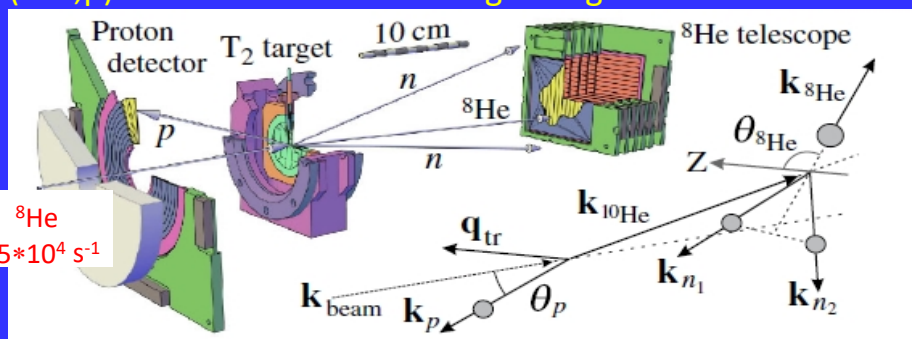
$$E_{\text{obs}} = 1.2 \pm 0.3 \text{ MeV}$$

$$\Gamma_{\text{obs}} \leq 1.2 \text{ MeV}$$

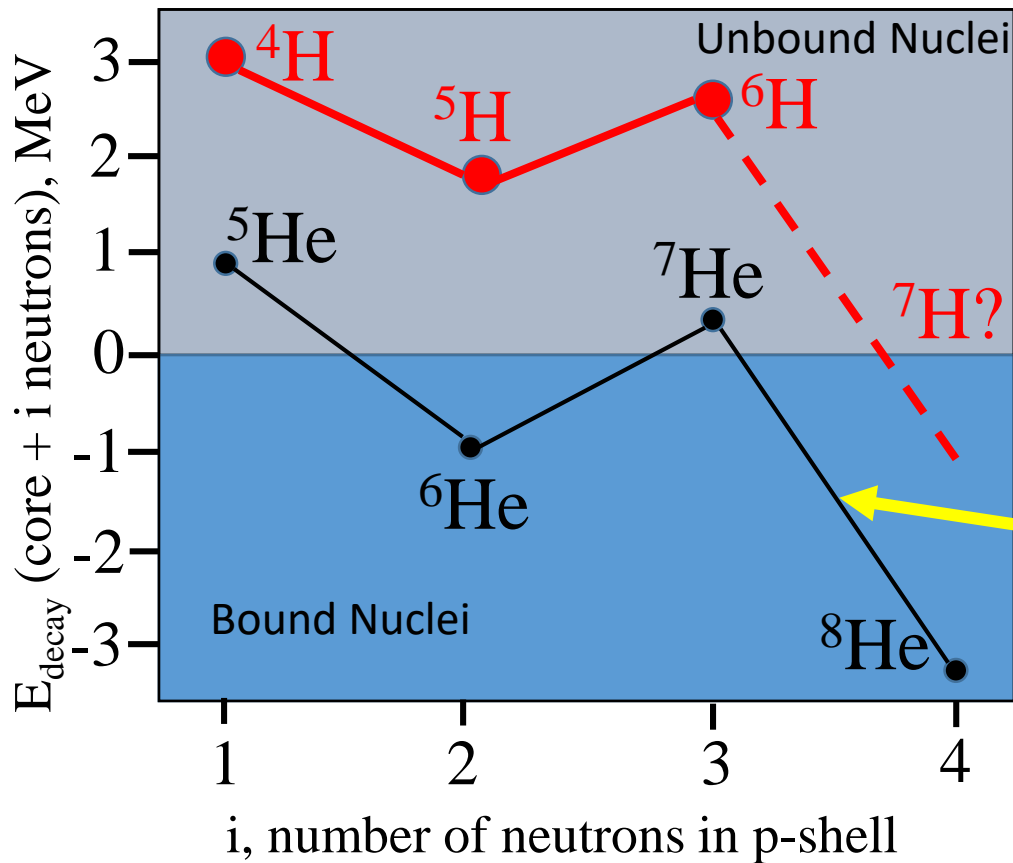
Z-axis: $\mathbf{q}_{\text{tr}} = -(1/4)\mathbf{k}_{\text{beam}} - \mathbf{k}_p$



$^3\text{H}(^8\text{He}, p)^{10}\text{He}$ reaction on tritium gas target with 21.5 AMeV ^8He beam



EXOTIC NUCLEI: Superheavy hydrogen isotopes ${}^{6,7}\text{H}$



The largest A/Z ratio !!

Unique many-body neutron decay channels !!

“Helium anomaly”

Theoretical calculations of ${}^7\text{H}(t+4n)$ energy:

E = 0.87 MeV (7-body hyperspherical functions)

N.K. Timofeyuk, PRC 65 064306 (2002)

E = 3 MeV (7-body hyperspherical functions, p.s.e.)

A.A. Korshennikov et al., PRL 90 082501 (2003)

E = 7 MeV (AMD)

S. Aoyama and N. Itogaki, NP A738 362 (2004)

Estimation of width of ${}^7\text{H}$: **$E \leq 3 \text{ MeV} \Leftrightarrow \Gamma \leq 1 \text{ MeV}$**

M.S. Golovkov et al., PL B588 163 (2004)

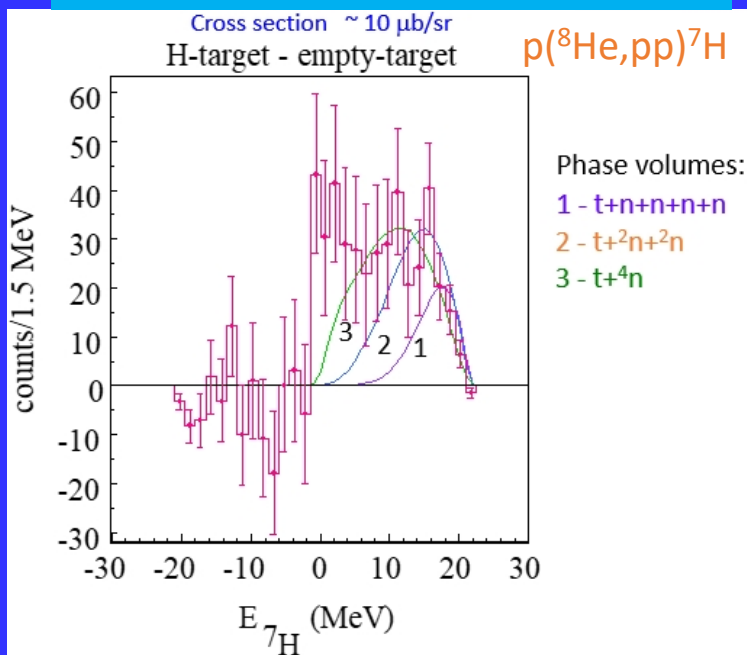
New Result:

$E \approx 9.5 \text{ MeV}$, $\Gamma = 3.5 \text{ MeV}$ (Variational Gaussian Expansion Approach)

E. Hiyama et al., PLB 833 137367 (2022)

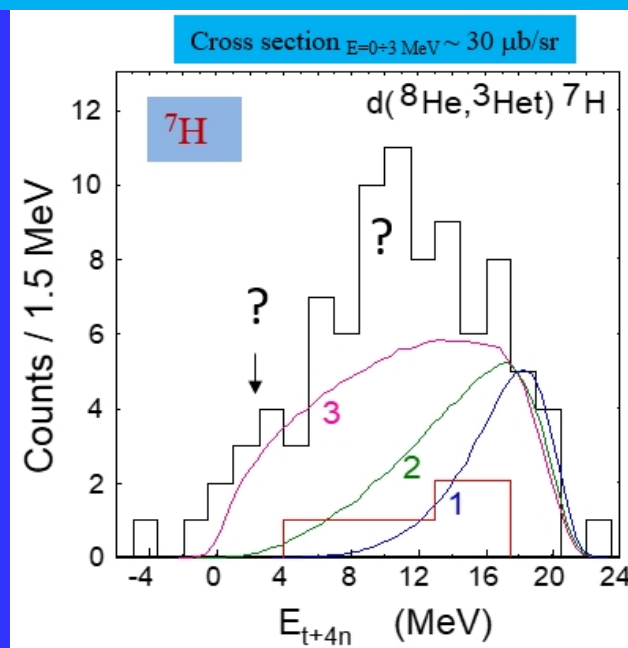
Experiments to search for ${}^7\text{H}$ states

1st RIKEN experiment to search for ${}^7\text{H}$

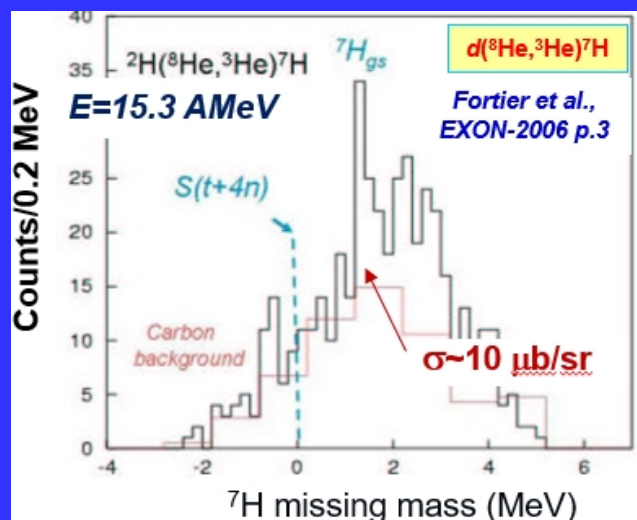


A. A. Korshennikov et al. PRL 90, 082501 (2003)

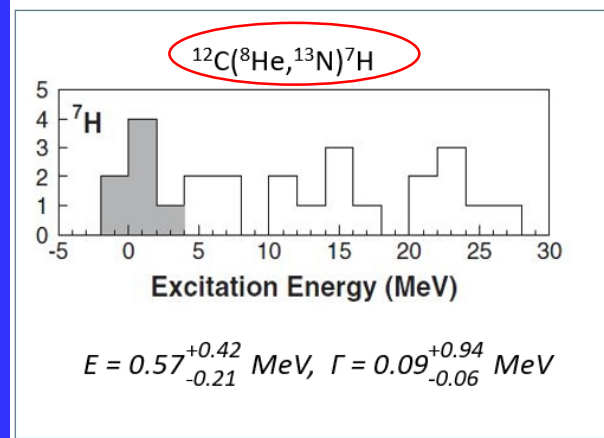
2nd RIKEN experiment to search for ${}^7\text{H}$



E.Yu.Nikolskii et al., PRC 81, 064606 (2010)



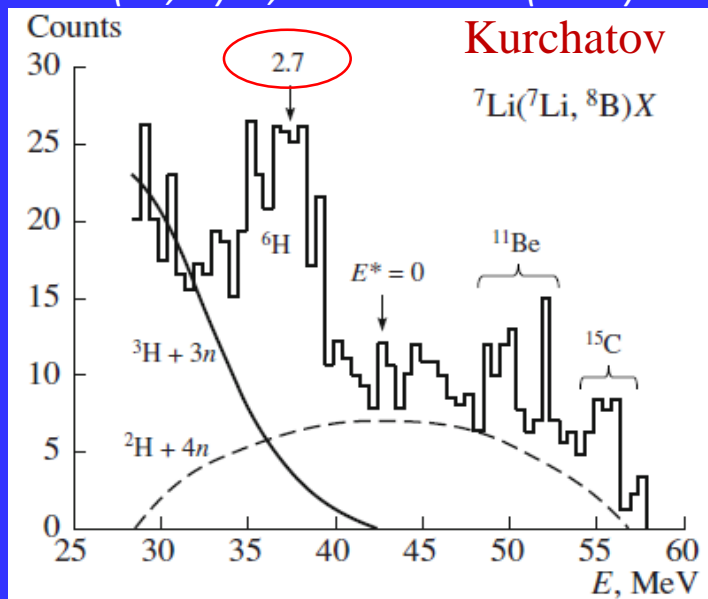
GANIL M. Caamaño et al.
 PRL 99, 062502 (2007)



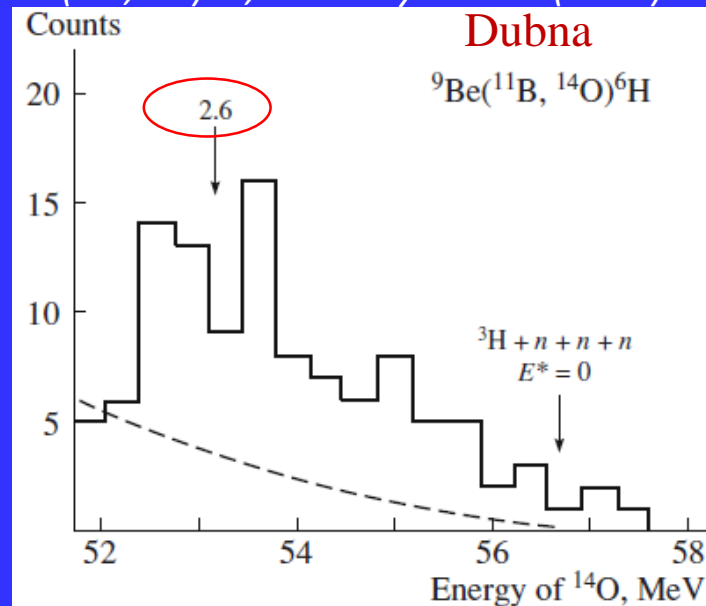
<i>Experiment</i>	<i>LAB</i>	<i>Energy (AMeV)</i>	<i>Result</i>	<i>Cross section ($\mu\text{b/sr}$)</i>
$p(^8\text{He}, pp)$	<i>RIKEN</i>	61	Very sharp increase from threshold No resonance parameters	~ 30 ($E \leq 3$ MeV)
$d(^8\text{He}, ^3\text{He})$	<i>GANIL</i>	15.3	Structure near 2 MeV No resonance parameters	—
$d(^8\text{He}, ^3\text{He})$	<i>Dubna</i>	25	Few events No resonance parameters	≤ 30 ($E \leq 3$ MeV)
$^{12}\text{C}(^8\text{He}, ^{13}\text{N})$	<i>GANIL</i>	15.3	7 events $E = 0.57^{+0.42}_{-0.21}$, $\Gamma = 0.09^{+0.94}_{-0.06}$ MeV	$40.1^{+58.0}_{-30.6}$
$d(^8\text{He}, ^3\text{He})$	<i>RIKEN new</i>	42	Abnormal shape near threshold, shoulder at ~ 2 MeV No resonance parameters	~ 30 ($E \leq 3$ MeV)

${}^6\text{H}$ search history

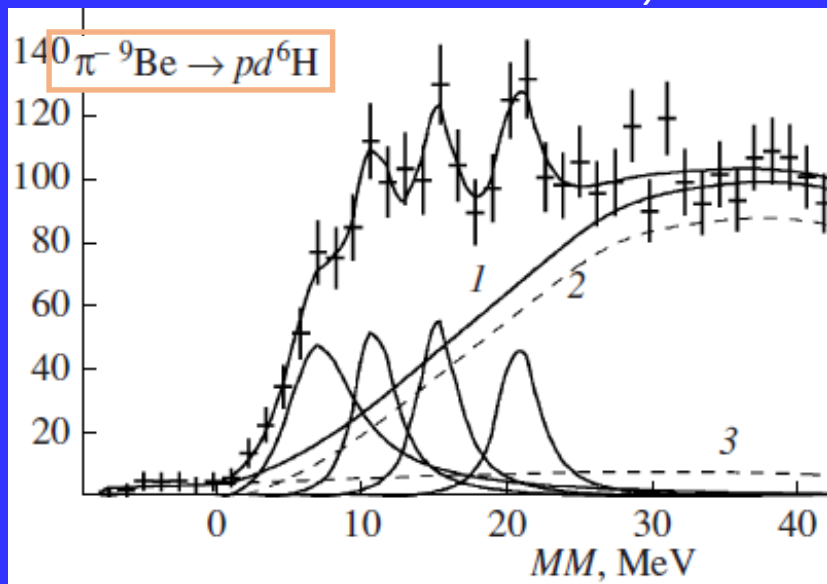
${}^7\text{Li}({}^7\text{Li}, {}^8\text{B}){}^6\text{H}$, *Yad.Fiz. m.39 (1984) 513*



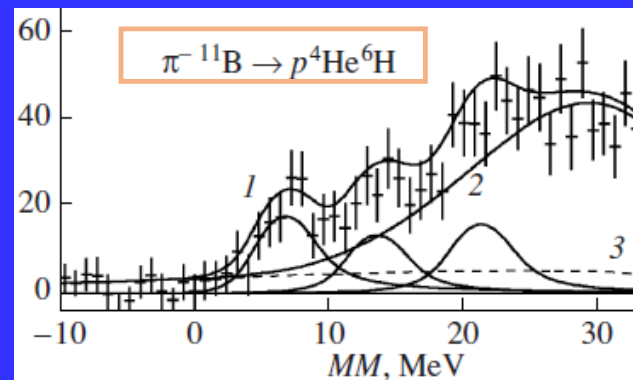
${}^9\text{Be}({}^{11}\text{B}, {}^{14}\text{O}){}^6\text{H}$, *Nucl.Phys. A460 (1986) 352*



Phys. Part. Nucl. 40 (1990) 558



${}^9\text{Be}(\pi^-, pd){}^6\text{H}$		${}^{11}\text{B}(\pi^-, p^4\text{He}){}^6\text{H}$	
E_r , MeV*	Γ , MeV**	E_r , MeV	Γ , MeV
6.6 ± 0.7	5.5 ± 2.0	7.3 ± 1.0	5.8 ± 2.0
10.7 ± 0.7	4 ± 2	-	-



ACCULINNA-2 separator layout (since 2017)

Cyclotron
U-400M



F1

D1

F2

D2

primary target

ACCULINNA-2

F3

RF
kicker

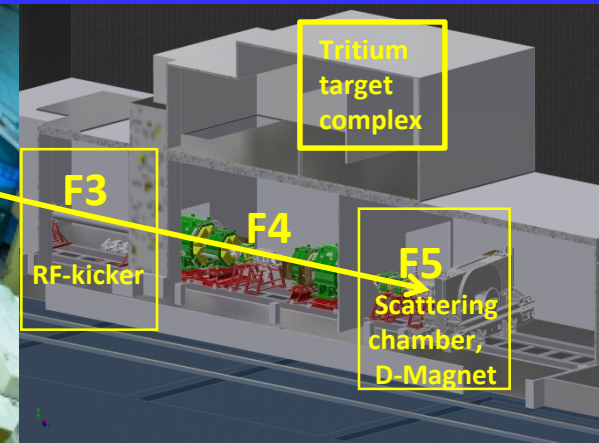
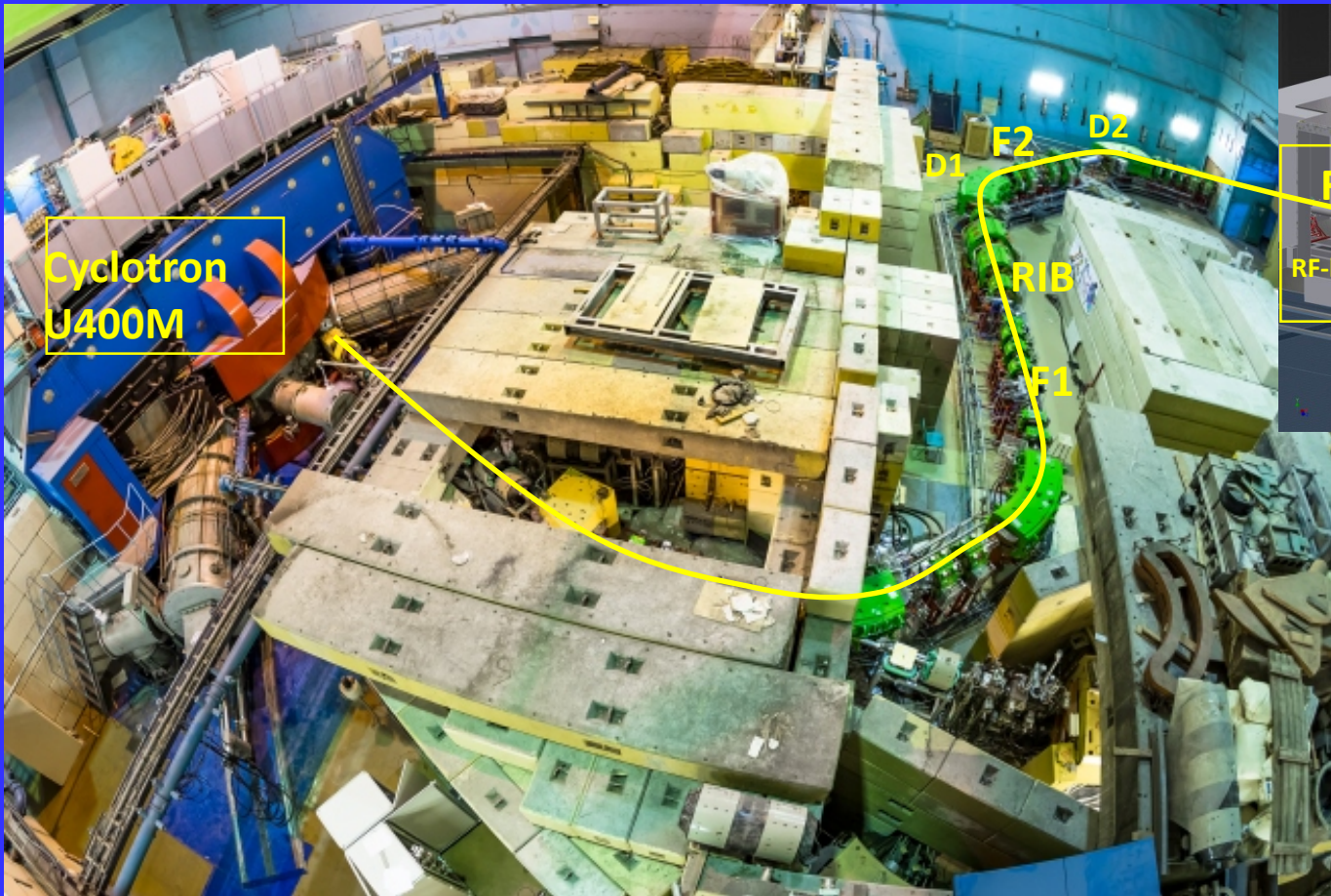
ACCULINNA

Zero-angle
spectrometer

F4

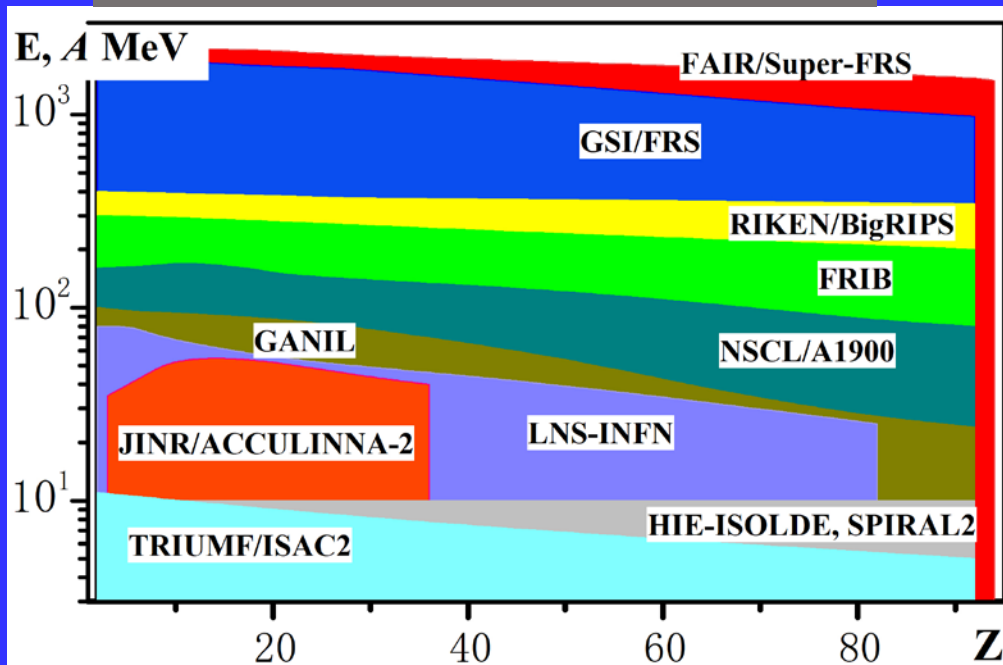
F5

physical target
(including tritium)
(~ end of 2024)



2011: Contract signed with Sigma PHI
2016-17: Full commissioning + Beam
2018-2019: First experiments
2020-2023: Upgrade U400M cyclotron

ACCULINNA-2 and world RIBs centers



Primary beams for ACCULINNA-2:

	I, μA
${}^6\text{Li}$ @ 46 AMeV	8
${}^{11}\text{B}$ @ 33 AMeV	5
${}^{15}\text{N}$ @ 50 AMeV	2
${}^{20}\text{Ne}$ @ 53 AMeV	1
${}^{32}\text{S}$ @ 52 AMeV	0.2

Secondary beams from ACCULINNA-2:

${}^{6,8}\text{He}$ @ 25÷35 AMeV
${}^{9,11}\text{Li}$ @ 30 AMeV
${}^{18}\text{Ne}$ @ 35 AMeV
${}^{28}\text{S}$ @ 38 AMeV
<i>In-flight separation</i>

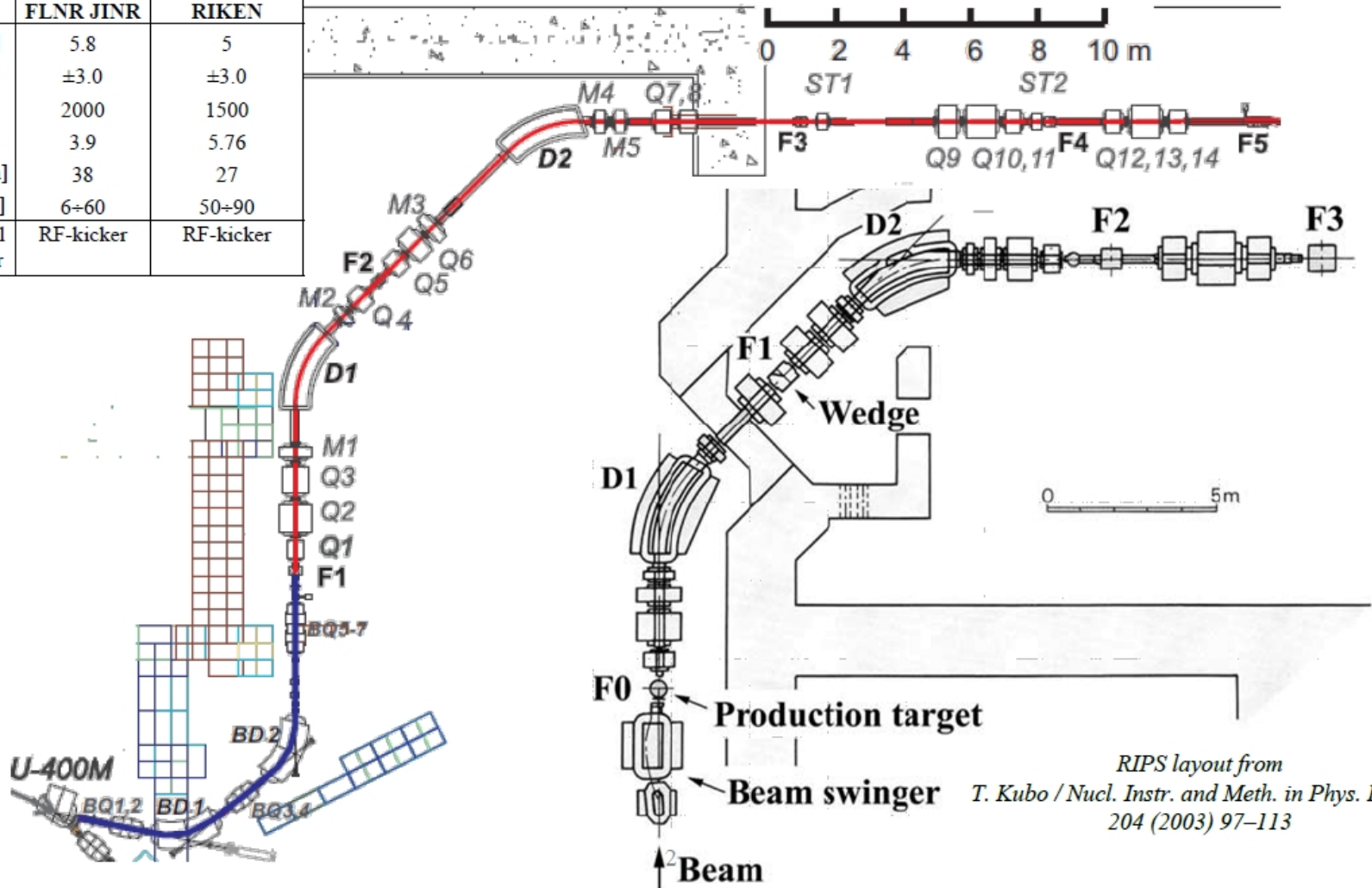
		ACC FLNR,	ACC-2 JINR	LISE3 GANIL	ARIS ^a FRIB	RIPS	BigRIPS RIKEN
$\Delta\Omega$	m sr	0.9	4.2	1.0	5.0	5.0	6.3
δ_P	%	2.5	6.0	5.0	10	6.0	6.0
$P/\Delta P$	a.u.	1000	2000	2200	4000	1500	3300
$B\rho_{max}$	Tm	3.2	3.9	3.2-4.3	8.0	5.76	9.0
Length	m	21	37	19(42)	87	21	77
E_{min}	AMeV	10	5	30	30 ^b	30	5 ^c
E_{max}	AMeV	40	50	80	300	90	350

ACCULINNA-2 is comparable with RIPS, RIKEN

Intensities of secondary beams ~ 15-25 times higher than ACCULINNA !!

ACCULINNA-2 layout compared to RIPS (RIKEN)

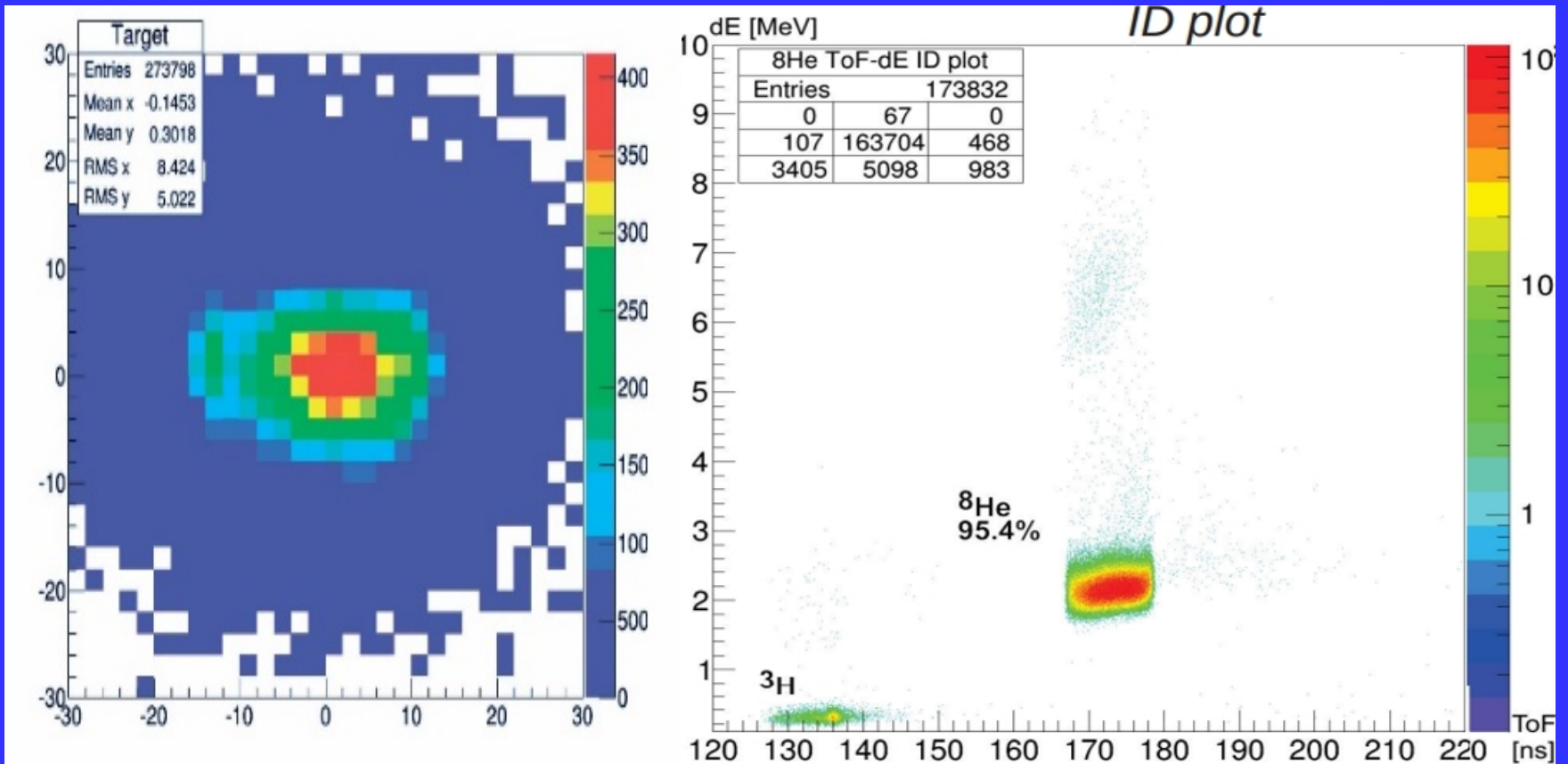
	ACC-2 FLNR JINR	RIPS RIKEN
$\Delta\Omega$ [msr]	5.8	5
$\Delta p/p$ [%]	± 3.0	± 3.0
$R_p/\Delta p$	2000	1500
B_p [Tm]	3.9	5.76
Length [m]	38	27
E [AMeV]	6+60	50+90
Additional RIB Filter	RF-kicker	RF-kicker



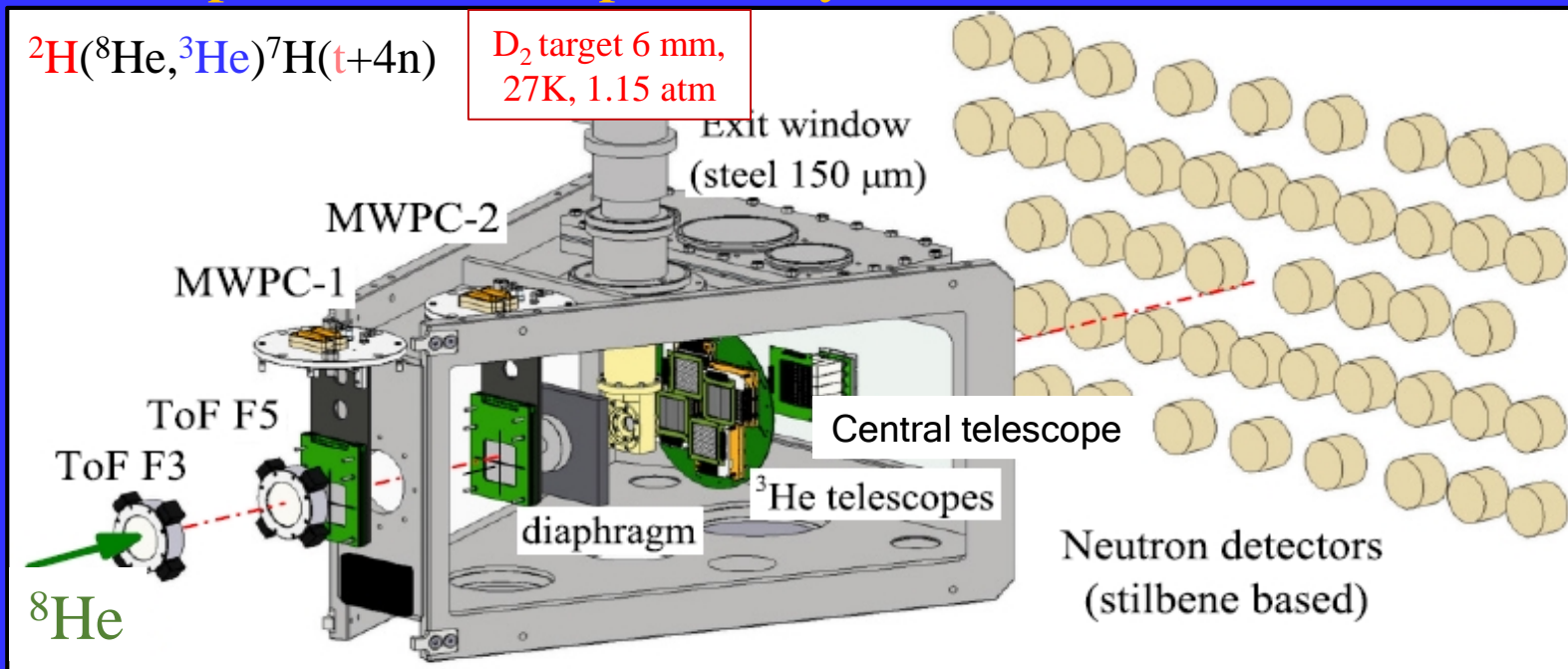
RIPS layout from
T. Kubo / Nucl. Instr. and Meth. in Phys. Res. B
204 (2003) 97-113

^8He beam

$I \sim 3 \cdot 10^5$ pps, $E \sim 26$ AMeV, $P > 90\%$, $\emptyset \sim 17$ mm

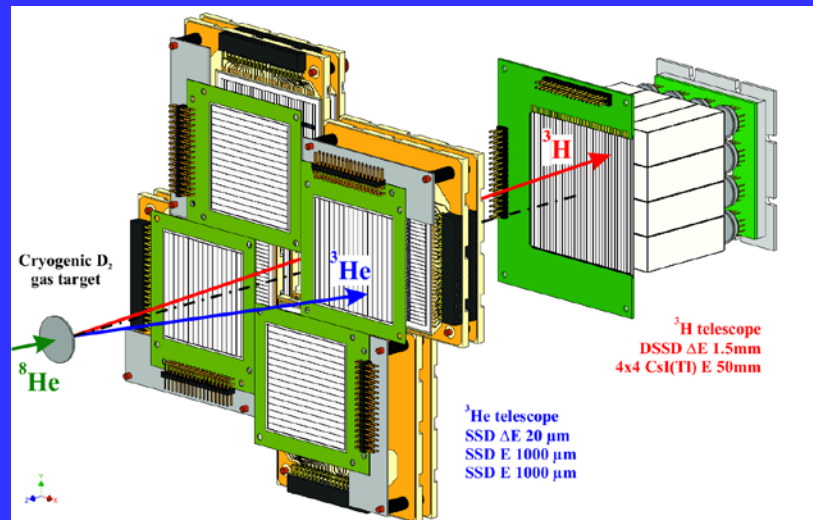
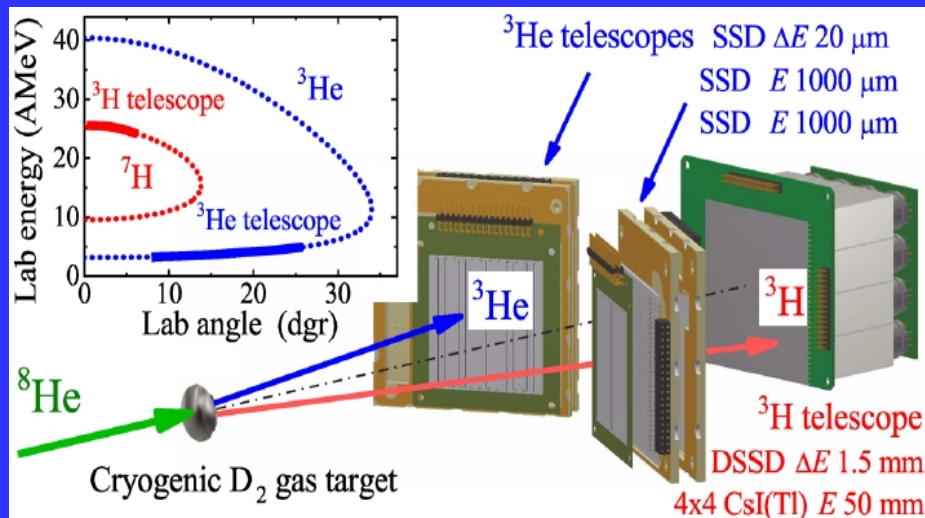


Experimental setup to study ${}^2\text{H}({}^8\text{He}, {}^3\text{He}){}^7\text{H}(t+4n)$ reaction



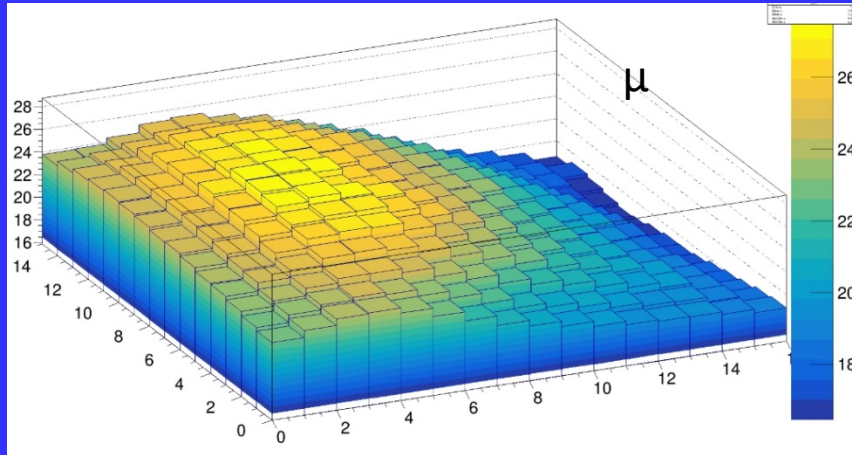
EXP 1, 2018 2 weeks, 107 ${}^7\text{H}$ (${}^3\text{He}+t$) events

EXP 2, 2019 3 weeks, 404 ${}^7\text{H}$ (${}^3\text{He}+t$) events

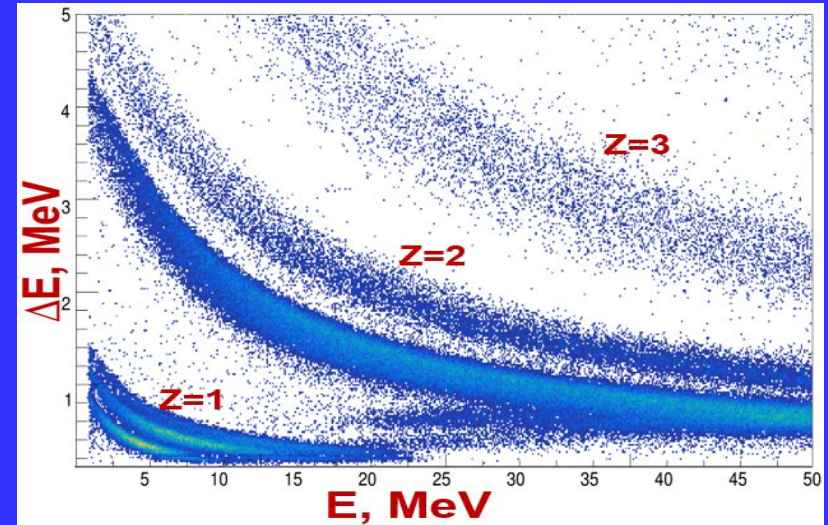


Identification of low-energy ^3He is a difficult task!

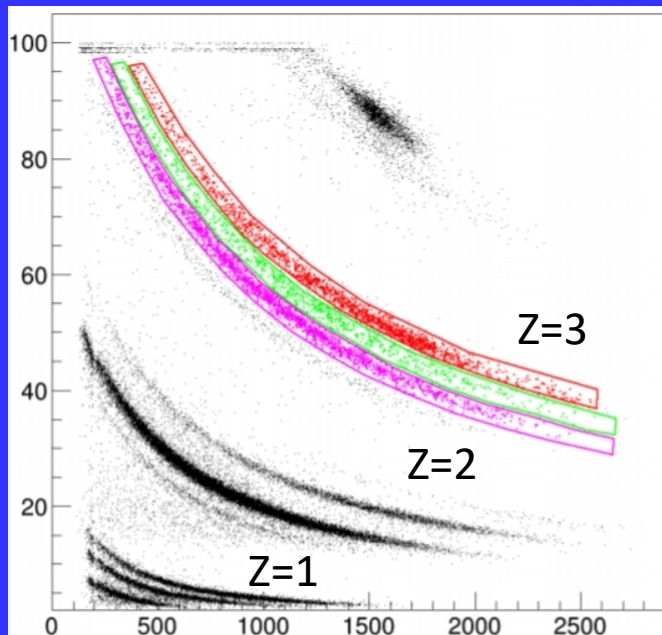
Measured thickness map of one of 20- μm detector



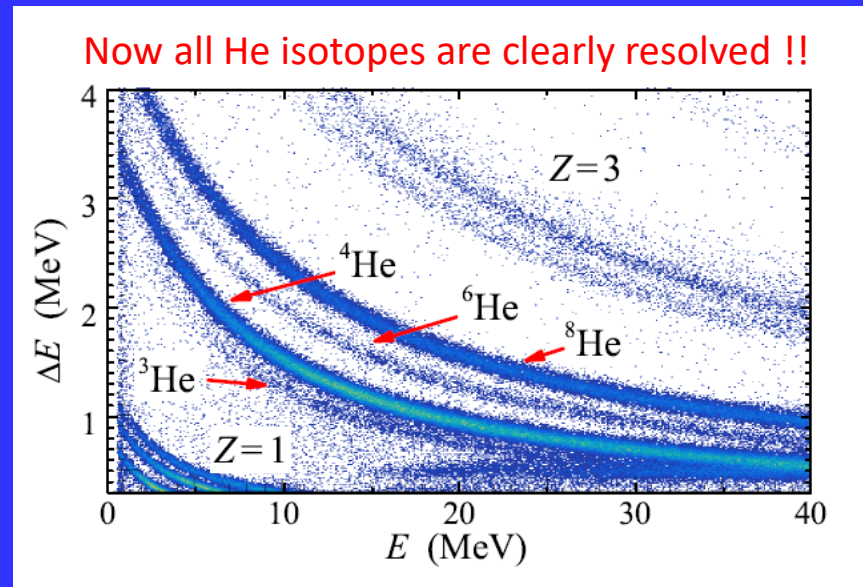
Particle ID w/o thickness correction of 20- μm detector



Identification in central telescope (^{10}Be beam)



Particle ID after thickness correction of 20- μm detector

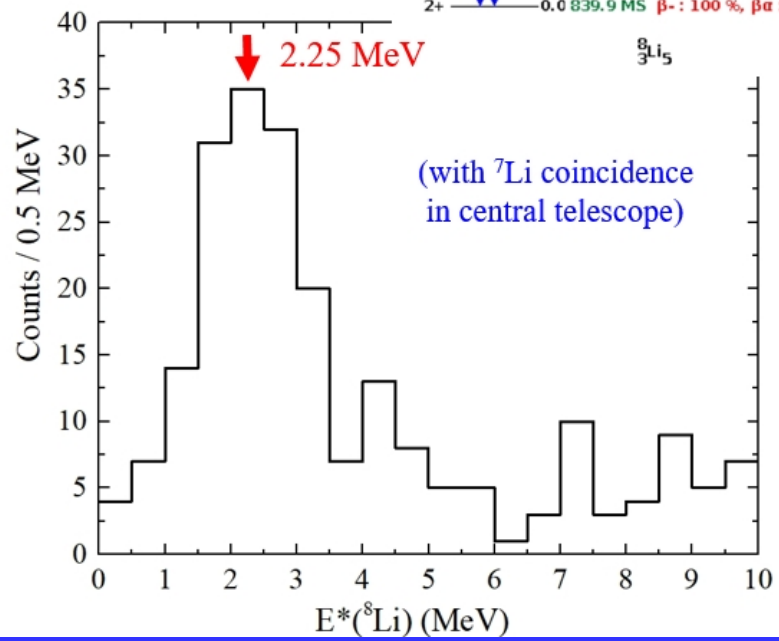
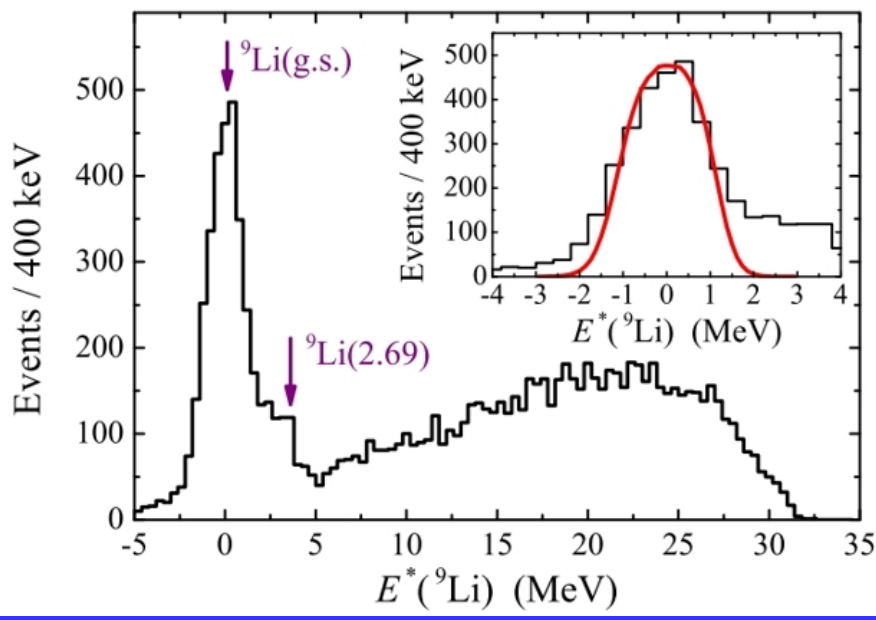
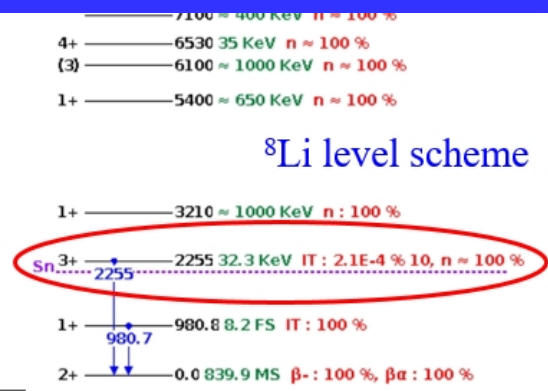
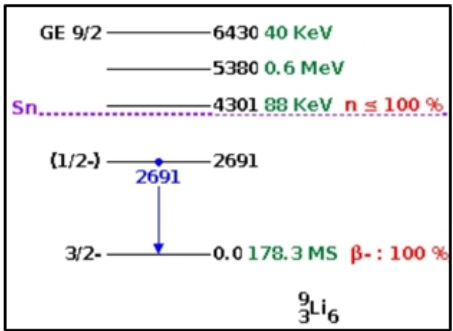


Now all He isotopes are clearly resolved !!

Test reactions ${}^2\text{H}({}^{10}\text{Be}, {}^3\text{He}){}^9\text{Li}$ and ${}^2\text{H}({}^{10}\text{Be}, {}^4\text{He}){}^8\text{Li}$ with 42 A MeV ${}^{10}\text{Be}$ beam

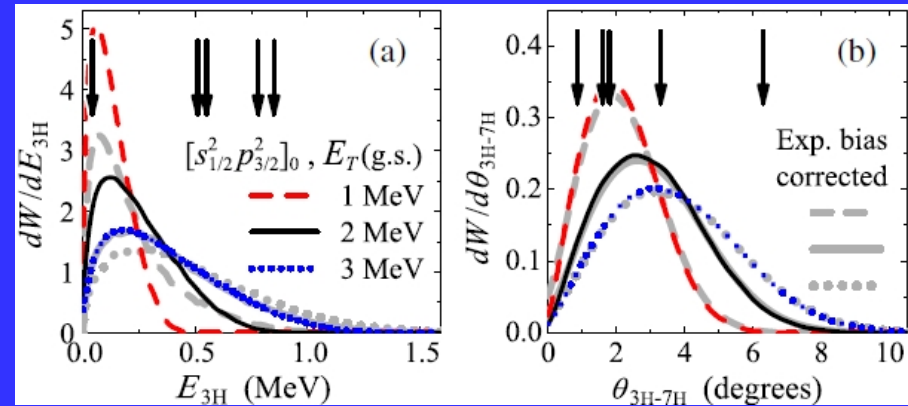
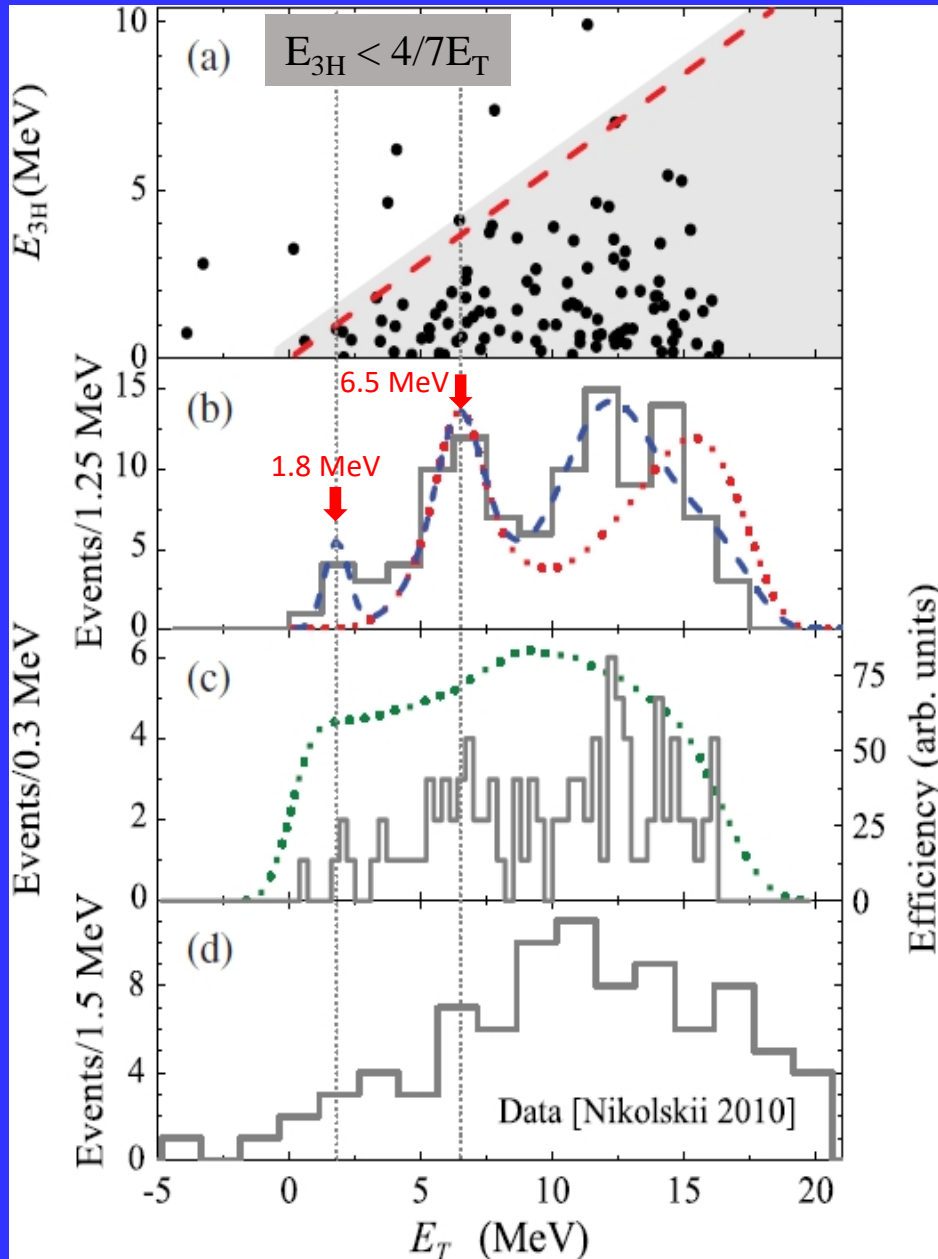
E. Yu. Nikolskii et al., NIMB 541 (2023) 121

Data for the reference reactions
 ${}^2\text{H}({}^{10}\text{Be}, {}^3\text{He}){}^9\text{Li}$ and ${}^2\text{H}({}^{10}\text{Be}, {}^4\text{He}){}^8\text{Li}$:
 * *energy calibration and resolution for the missing mass spectra;*
 ** *detector efficiency;*

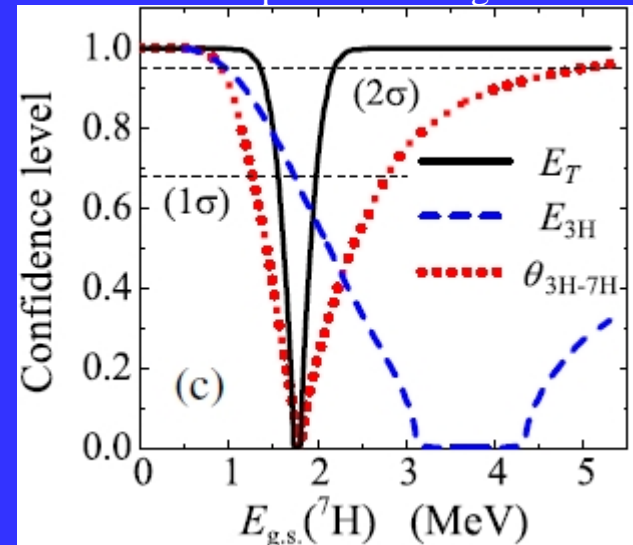


Detailed data of ${}^7\text{H}$ of the 1st Run

[A.A. Bezbakh *et al.*, PRL 124, 022502 (2020)]



MC likelihood functions of confidence level for the position of ${}^7\text{Hg.s.}$



Indication of the $1/2^+$ g.s. of ${}^7\text{H}$ at $E = 1.8(5)$ MeV with $cs \sim 25 \mu\text{b}/\text{sr}$ at $\theta_{\text{cm}} \approx 17^\circ - 27^\circ$

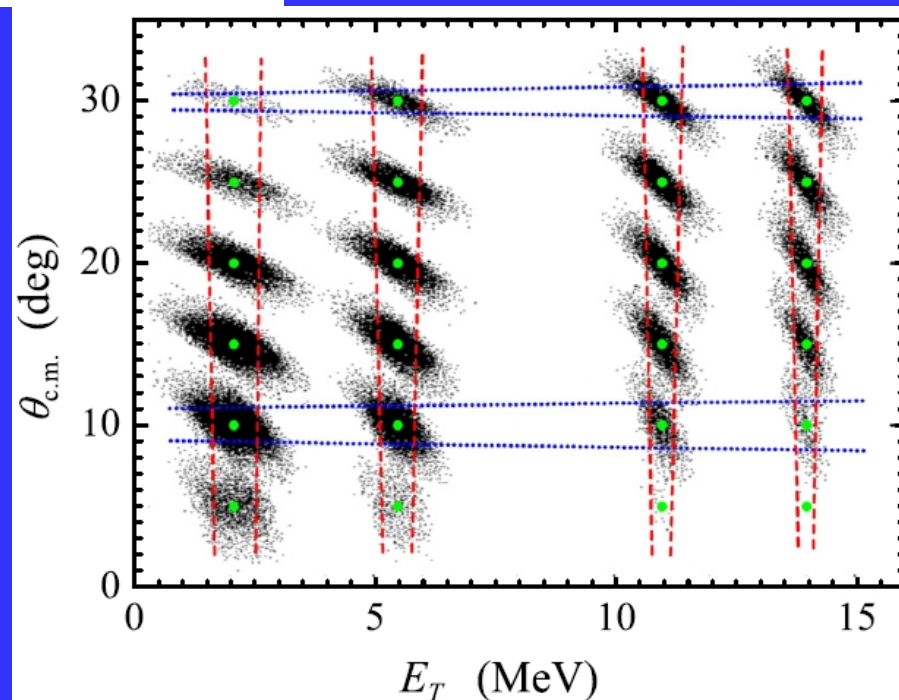
Conclusion after 1st Run:

(i) For the first time, the ${}^7\text{H}$ excited state is observed at $E_T = 6.5(5)$ MeV with $\Gamma = 2.0(5)$ MeV. This state can be interpreted as the unresolved $5/2+$ and $3/2+$ doublet built upon the $2+$ excitation of valence neutrons, or one of the doublet states.

(ii) Indications for the ${}^7\text{Hg.s.}$ at $E_T = 1.8(5)$ MeV are found in the measured energy and angular distributions. The cross section obtained for the presumed ${}^7\text{Hg.s.}$ populated in the ${}^8\text{He}(d, {}^3\text{He}){}^7\text{H}$ reaction in the $\Theta_{\text{CM}} = 7^\circ - 27^\circ$ is ≈ 25 $\mu\text{b/sr}$. This corresponds to a weak population of the g.s. with experimental SF ~ 0.1 , which clarifies why the previous searches for the ${}^7\text{Hg.s.}$ required so much time and efforts without bringing reliable assignments of such a remote isotope.

TABLE I. Experimental resolution in the second experiment as a function of the ${}^7\text{H}$ MM energy and center-of-mass angle $\theta_{\text{c.m.}}$, based on the MC simulations Fig. 8. The first and second values in each cell are the FWHM energy and the angular resolutions given in MeV and degrees, respectively.

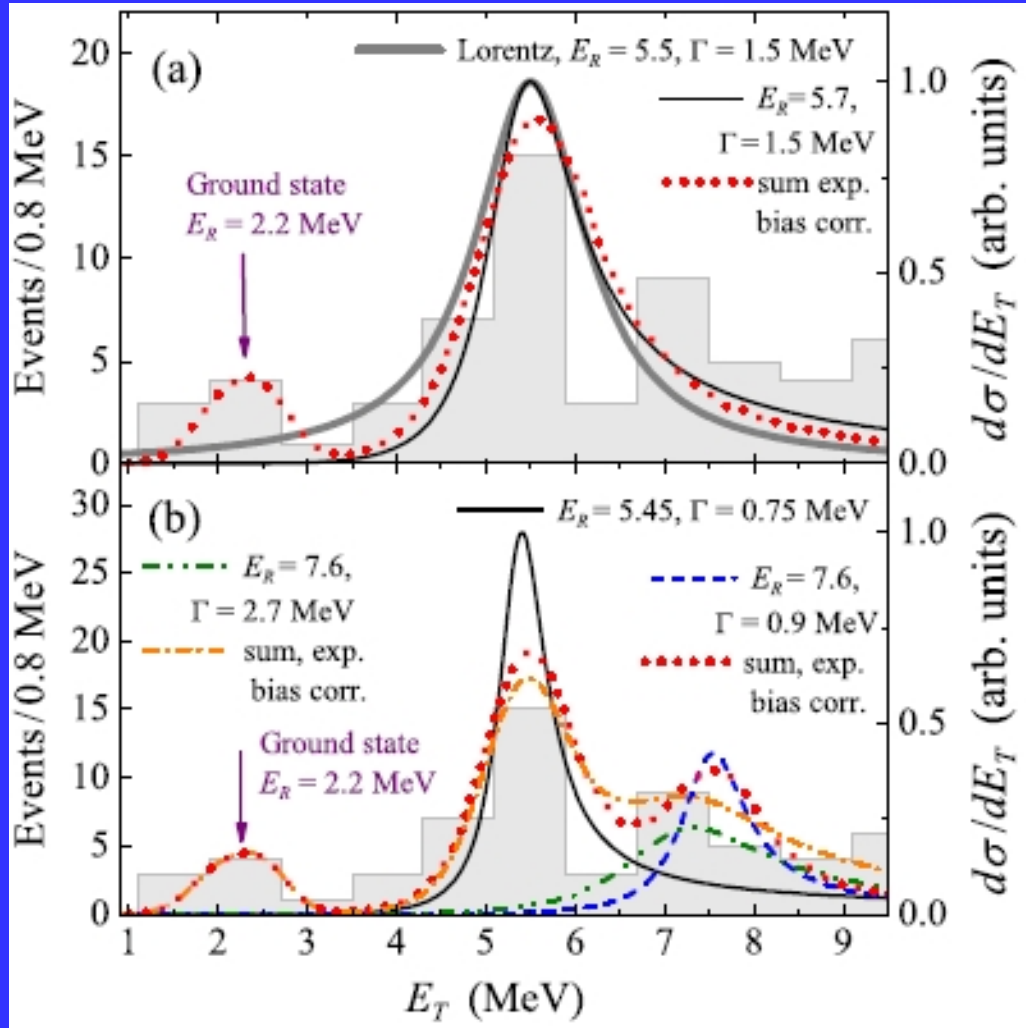
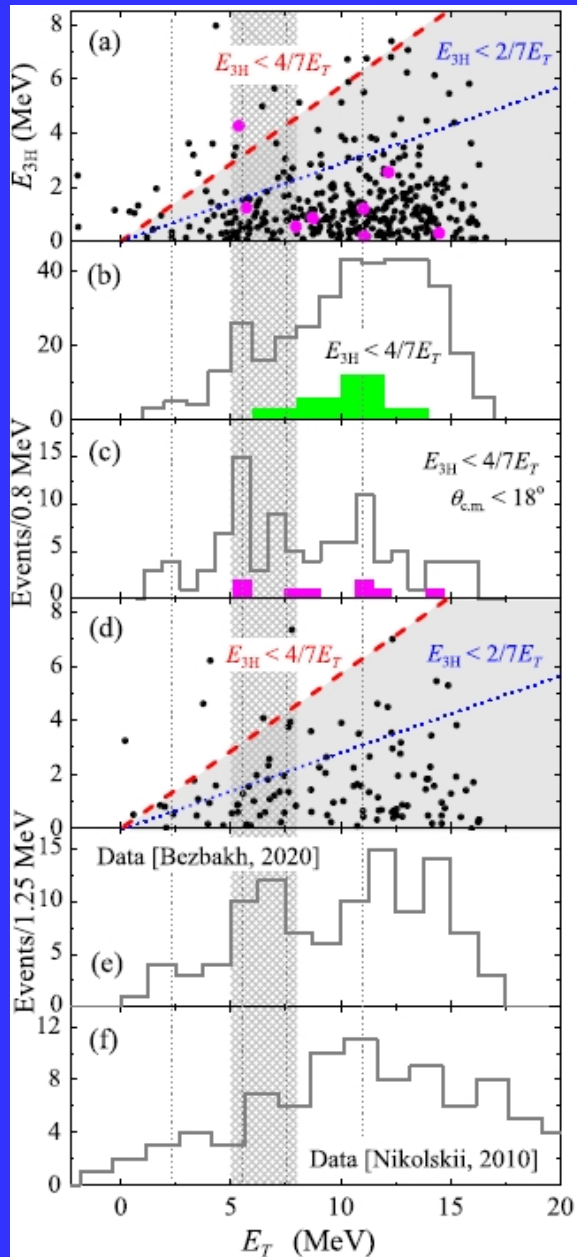
E_T	2.2 MeV		5.5 MeV		11 MeV		14 MeV	
10°	0.95	2.2	0.73	2.3	0.48	2.5	0.38	2.8
20°	1.10	1.6	0.93	1.8	0.64	2.2	0.52	2.6
30°	1.13	1.2	0.99	1.3	0.77	1.8	0.69	2.0



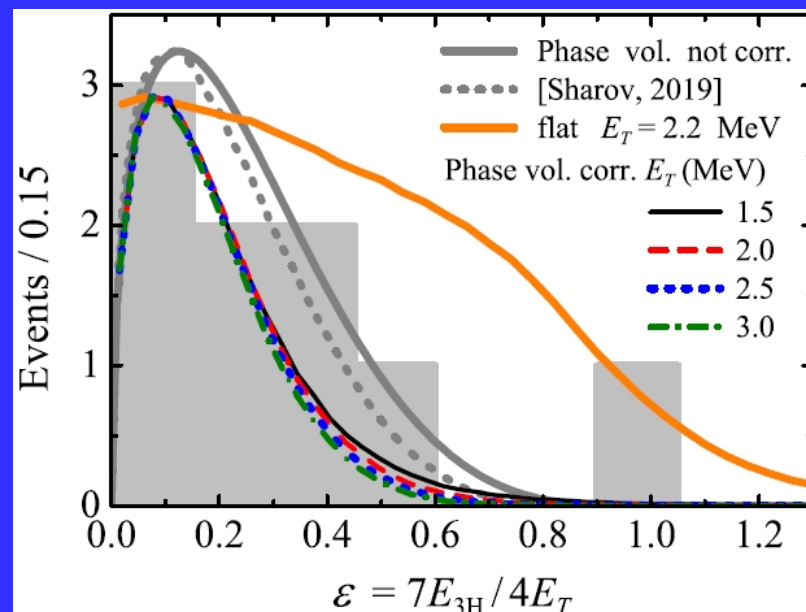
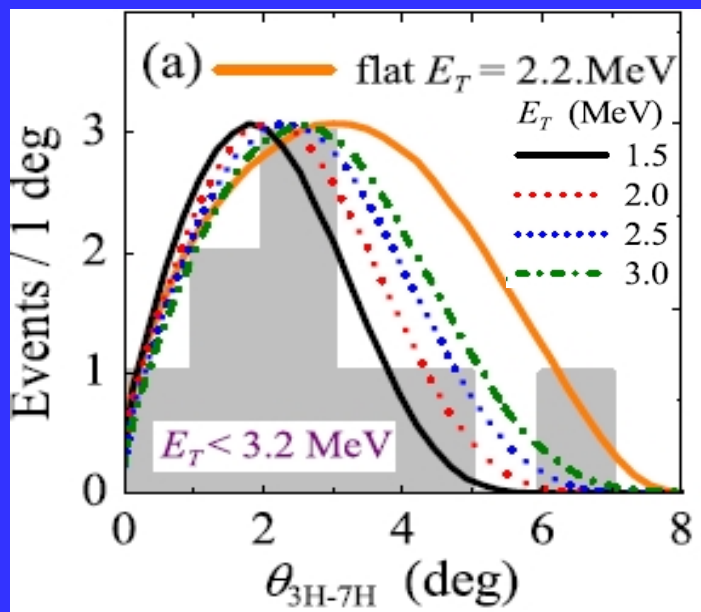
Detailed data of ${}^7\text{H}$ of the 2nd Run

[I. A. Muzalevskii et al, PRC 103, 044313 (2021)]

${}^7\text{H}$ spectrum after $E_{3\text{H}} < 4/7E_T$ and $\Theta_{\text{CM}} < 18^\circ$ selections



Additional support for the position of ${}^7\text{Hg.s.}$ at $E = 2.2(5)\text{MeV}$ comes from the angular and energy distributions of tritons from the ${}^7\text{H}$ decay for the events $E_T < 3.2\text{ MeV}$



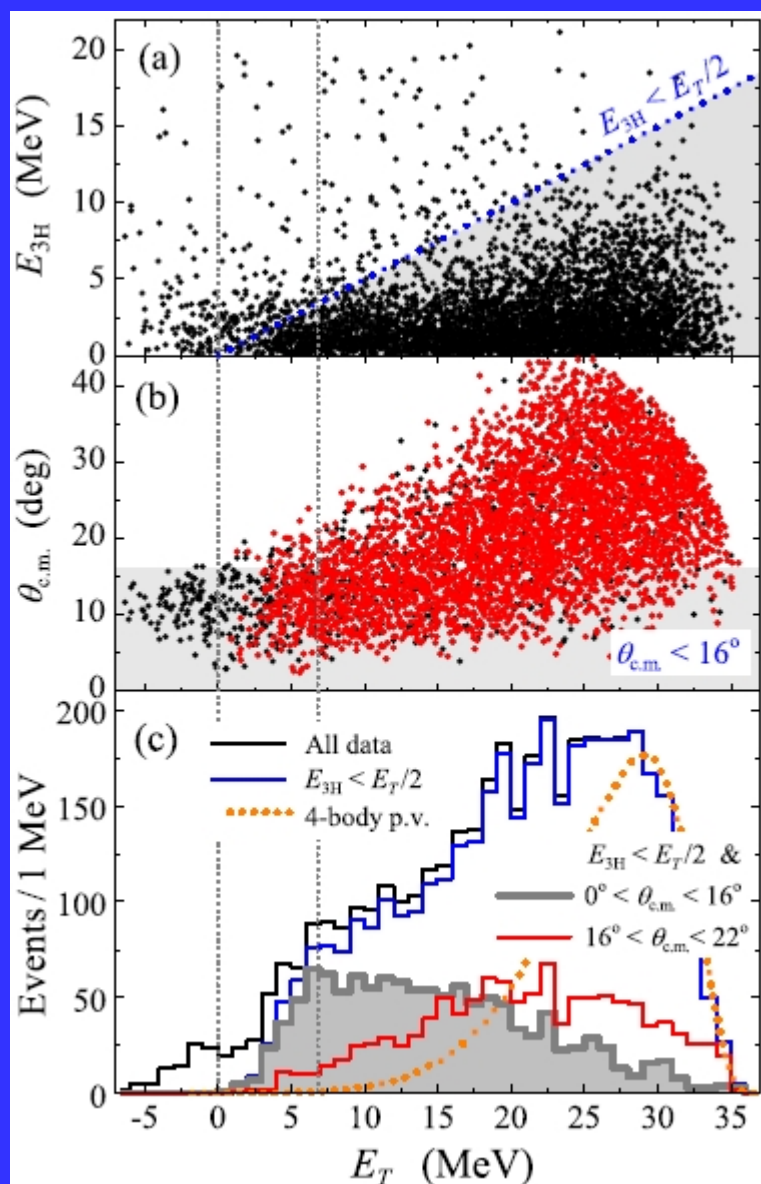
Value	flat	1.5	2.0	2.5	3.0	Expt.
$\langle \varepsilon \rangle$	0.46(11)	0.28(6)	0.26(6)	0.24(6)	0.23(6)	0.31
$\langle \theta_{3\text{H}-7\text{H}} \rangle$	3.5(6)	2.3(4)	2.6(4)	2.8(4)	3.0(4)	2.9

The value ε is consistent with $E_T < 2.2\text{ MeV}$. The best fit to the experimental $\langle \theta_{3\text{H}-7\text{H}} \rangle$ value is obtained at $E_T = 2.6(7)\text{ MeV}$. Both values are consistent with $E_T = 2.2(5)\text{ MeV}$ inferred from the MM data.

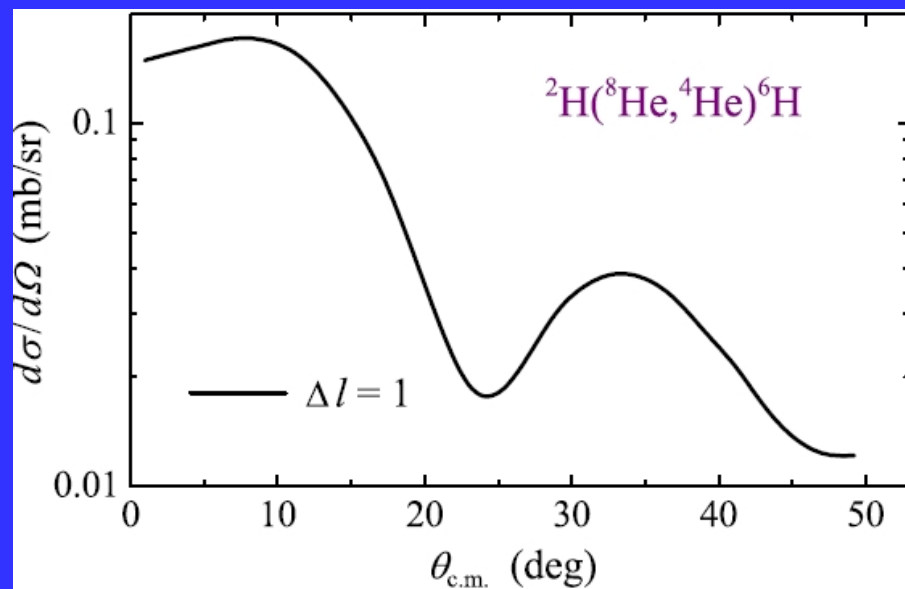
Conclusion after 1st and 2nd experiments:

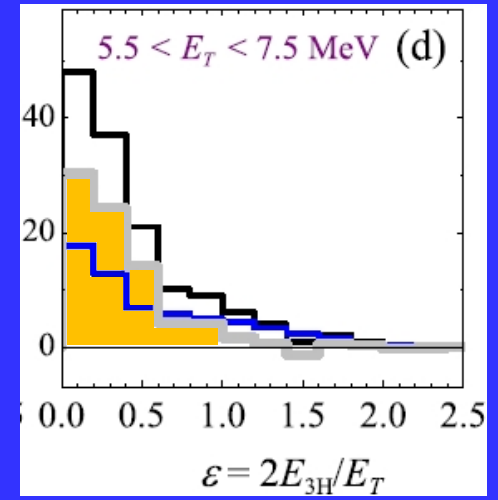
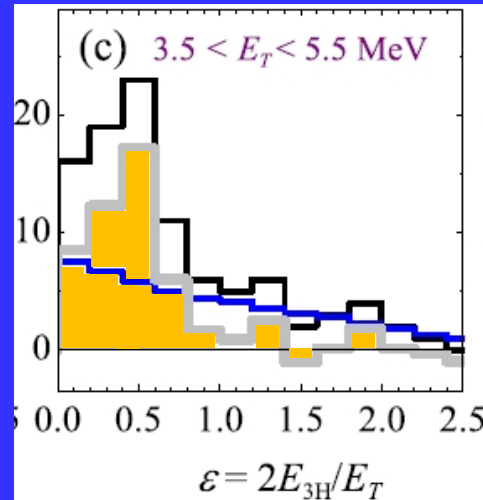
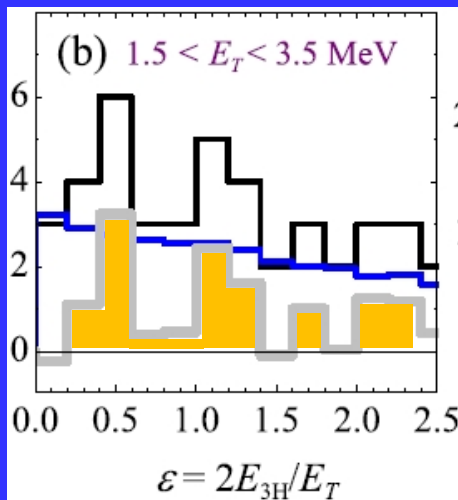
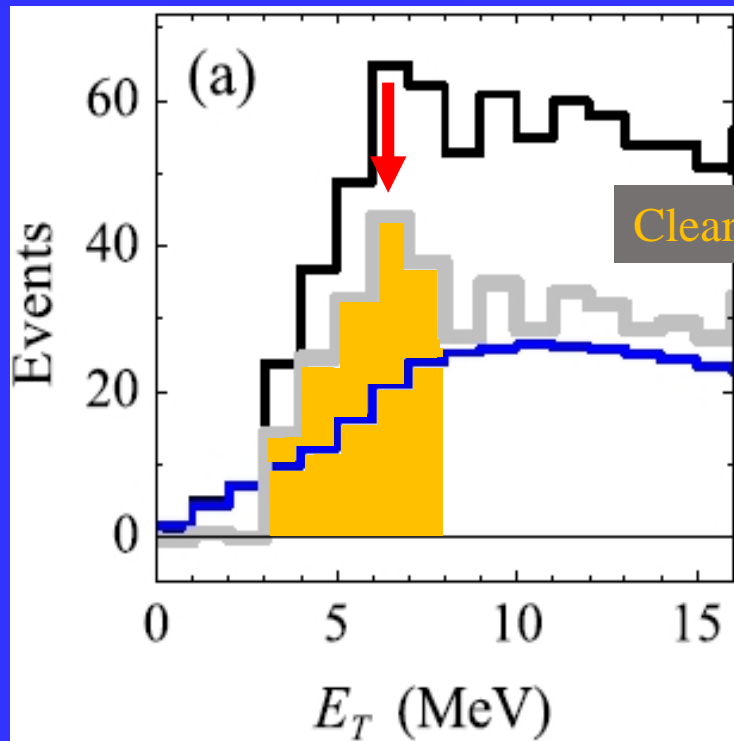
1. A solid experimental evidence is provided that two resonant states of ${}^7\text{H}$ are located in its spectrum at **2.2(5)** and **5.5(3) MeV** relative to the ${}^3\text{H}+4\text{n}$ decay threshold.
2. Based on the energy and angular distributions, obtained for the ${}^2\text{H}({}^8\text{He}, {}^3\text{He}){}^7\text{H}$ reaction, the weakly populated **2.2(5)-MeV peak** is ascribed to the ${}^7\text{H}$ $1/2^+$ **ground state**.
3. There are indications that the resonant states at **7.5(3)** and **11.0(3) MeV** are present in the measured ${}^7\text{H}$ spectrum.
4. It is highly plausible that the firmly ascertained **5.5(3)-MeV** state is the $5/2^+$ member of the ${}^7\text{H}$ excitation **$5/2^+ - 3/2^+$ doublet**, built on the 2^+ configuration of valence neutrons. The supposed **7.5-MeV state** can be another member of this doublet, which could not be resolved in 1st Run.

Study of ${}^6\text{H}$ system by measuring the ${}^2\text{H}({}^8\text{He}, {}^4\text{He}){}^6\text{H} \rightarrow \text{t} + 3\text{n}$ reaction

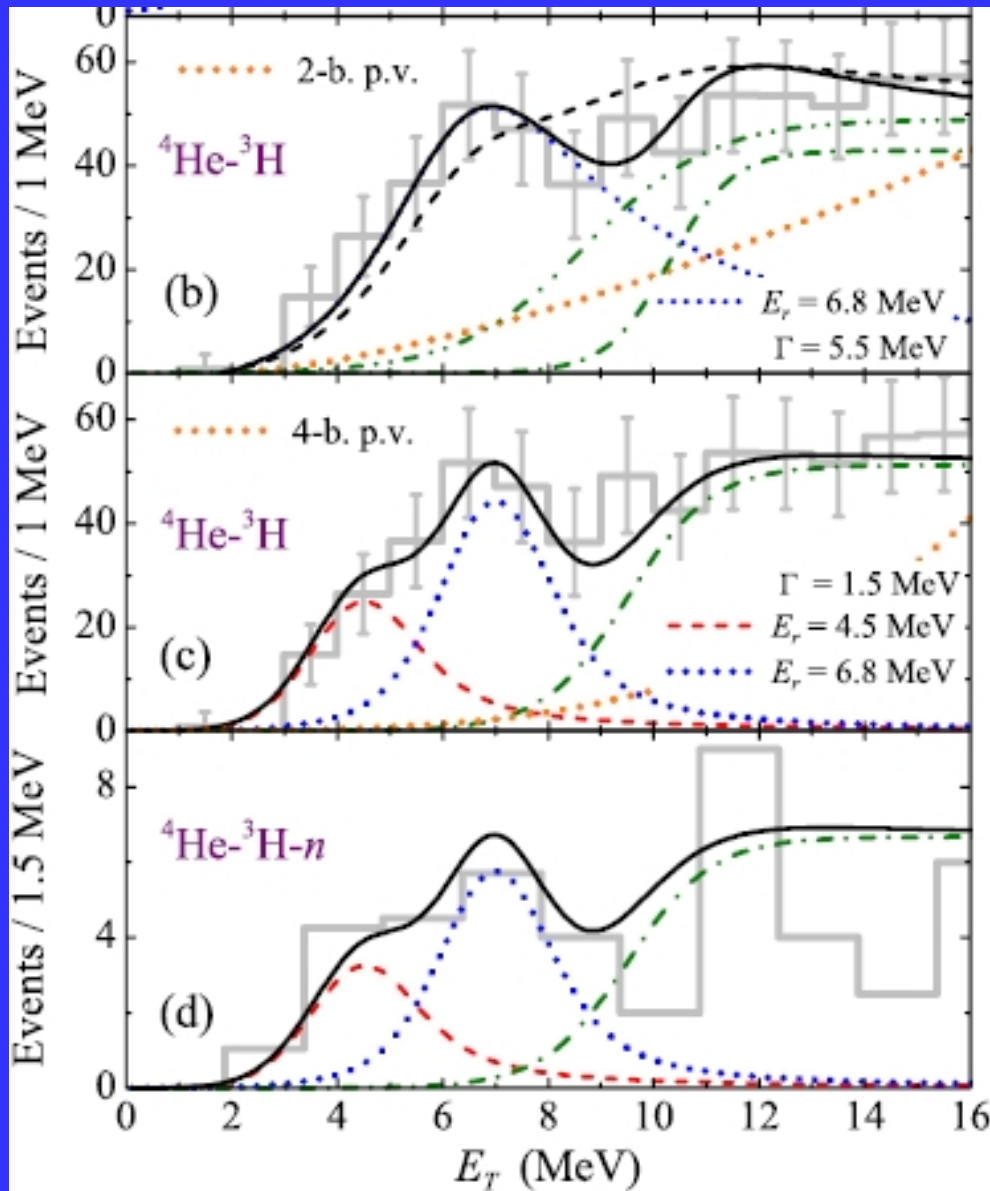


The $\Delta L = 1$ cross section for the ${}^2\text{H}({}^8\text{He}, {}^4\text{He}){}^6\text{H}$ reaction obtained in FRESKO calculations





Final ${}^6\text{H}$ spectra corrected for the experimental efficiency
with cutoff $\Theta_{\text{CM}} < 16^\circ$



$$\frac{d\sigma}{dE_T} \approx \frac{\Gamma(E_T)}{(E_r - E_T)^2 + \Gamma(E_T)^2/4}$$

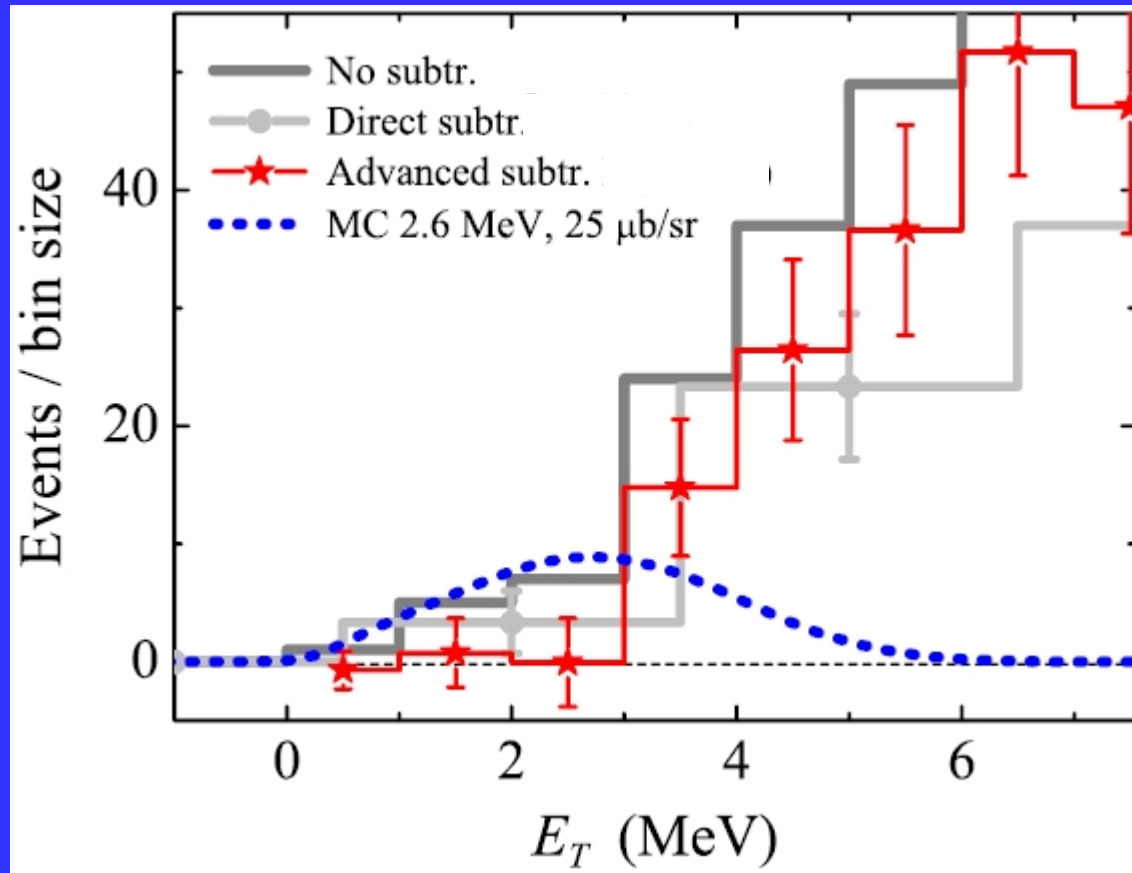
One state interpretation

Two states interpretation

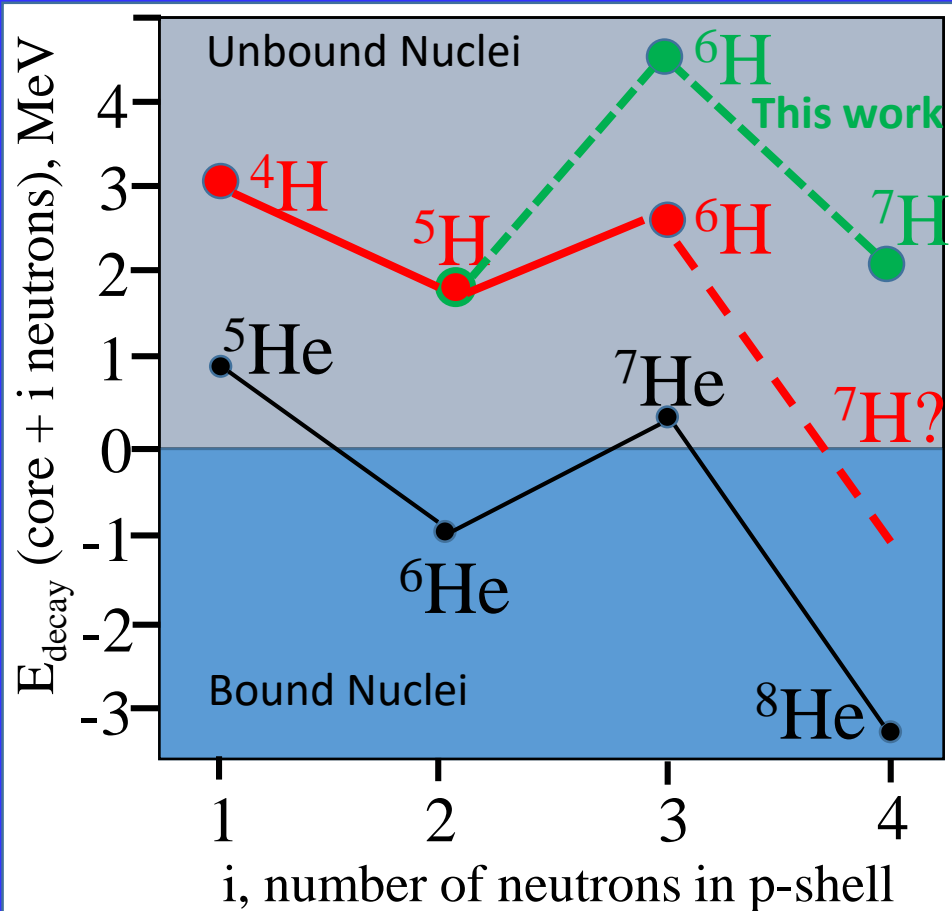
Two states interpretation with
neutron coincidences

No indications for the ${}^6\text{H}$ state at $E \sim 2.7 \text{ MeV}$ with cross section limit $d\sigma/d\Omega_{\text{CM}} \leq 5 \mu\text{b/sr}$!!

Instead, we observed the population cross section of $d\sigma/d\Omega_{\text{CM}} \approx 190 \mu\text{b/sr}$ for the **6.8 MeV broad state** at angular range $5^\circ < \Theta_{\text{CM}} < 16^\circ$

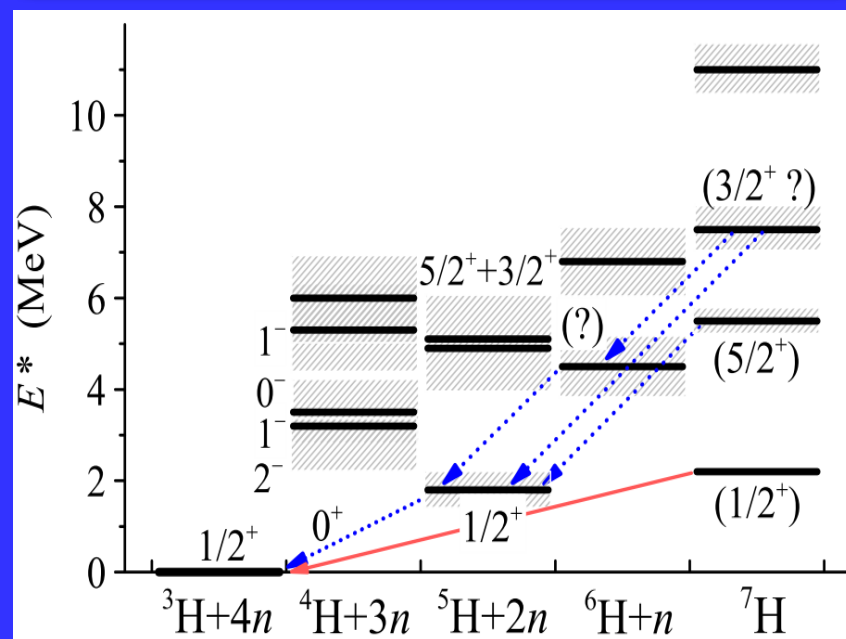


Hydrogen and helium chains: today status

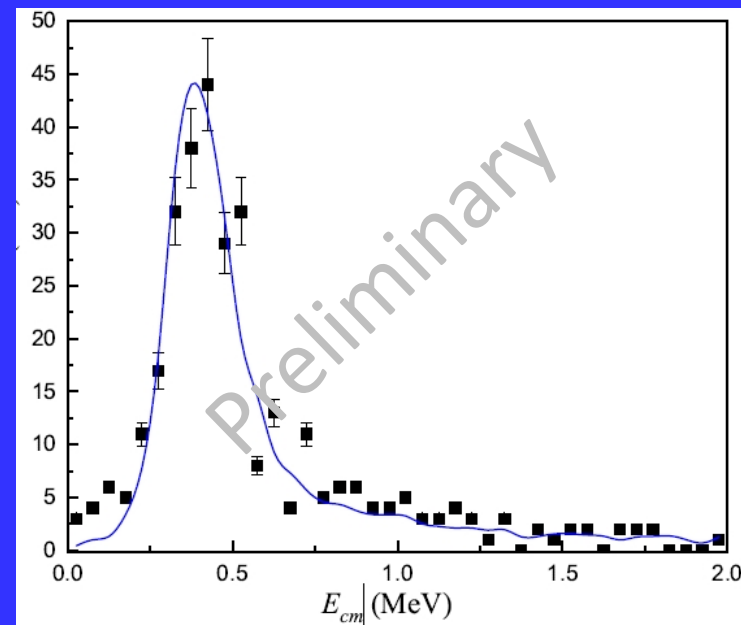
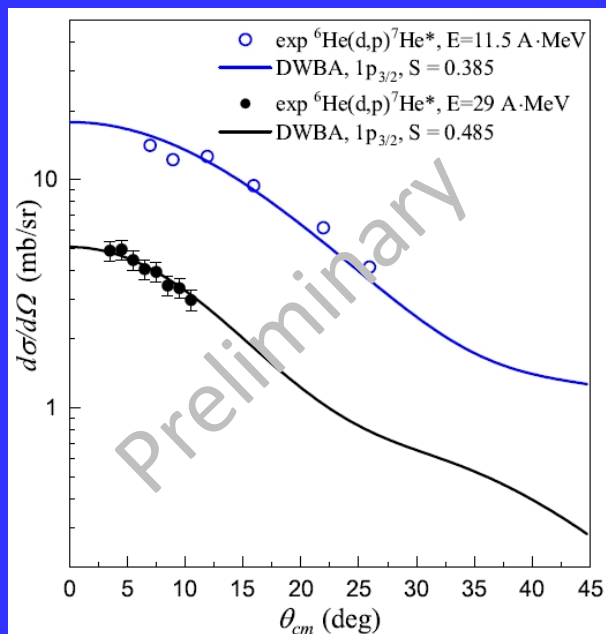
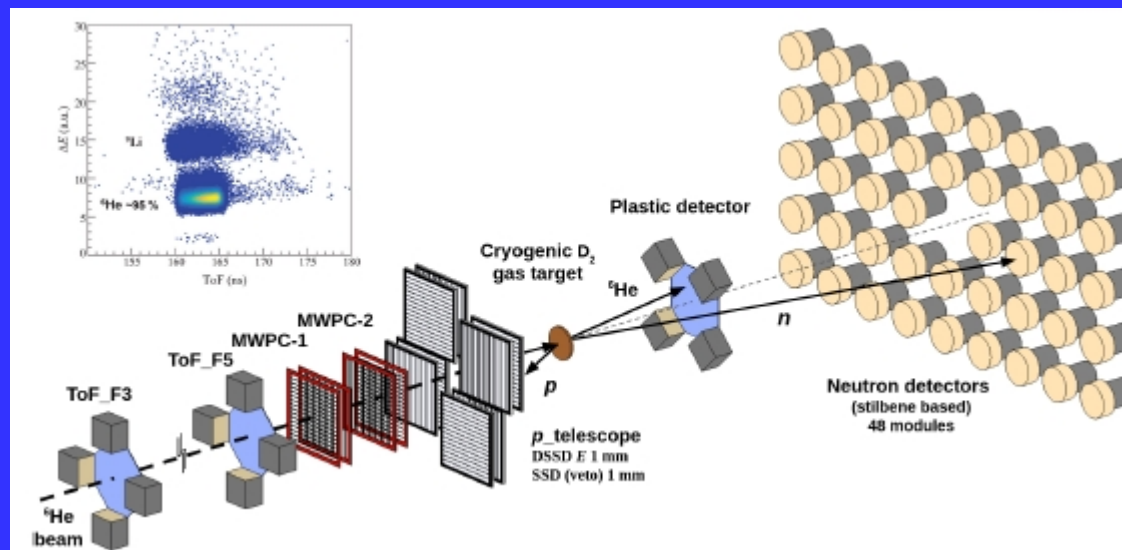


* New level schemes for chain $^4\text{H} \div ^7\text{H}$

** The unique true $4n$ -decay mechanism is proved to be realized for ^7H . This is the first such case found in the nuclide map.



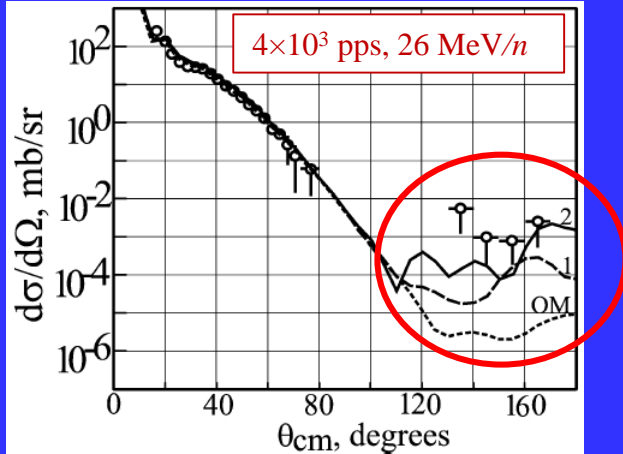
${}^7\text{He}$ spectrum studied by the ${}^6\text{He}(d,p){}^7\text{He}$ reaction



Going ahead...

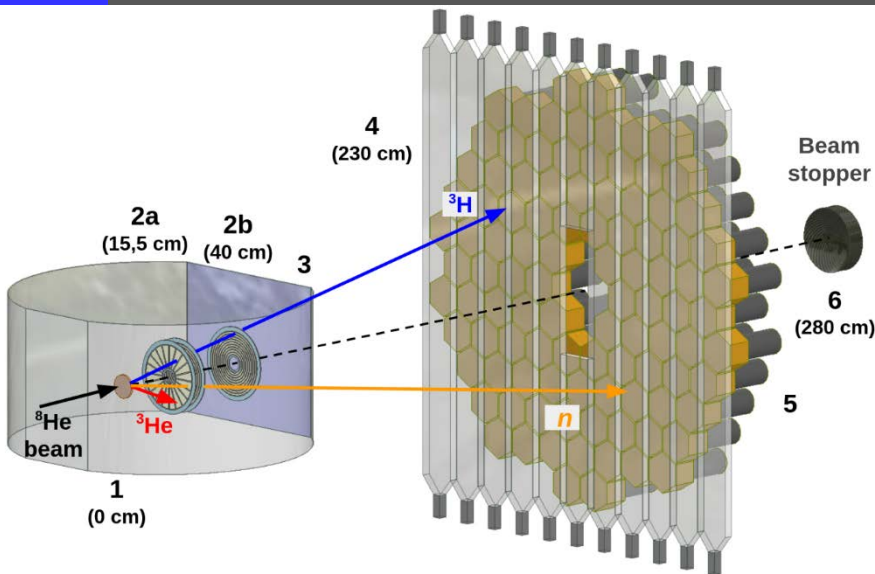
Search for 4n transfer in the $^8\text{He}+^4\text{He}$ scattering

R. Wolski et al., Nucl. Phys. A **701** (2002) 29c



~ 5 counts per 10 days are expected for the $^8\text{He}+^4\text{He}$ elastic scattering at $d\sigma/d\Omega = 10^{-5}$ mb/sr in the θ_{cm} range $150^\circ - 175^\circ$

Isobar-analogue states in ^5H and ^5He in the $^6\text{He}+d$ collisions



Invariant mass measurements

D_2 target $1 \times 10^{21} \text{ cm}^{-2}$

85 counts per 10 days for $^3\text{He}+t+2n$ events

FWHM resolution of ~ 400 keV

Going ahead... (2)

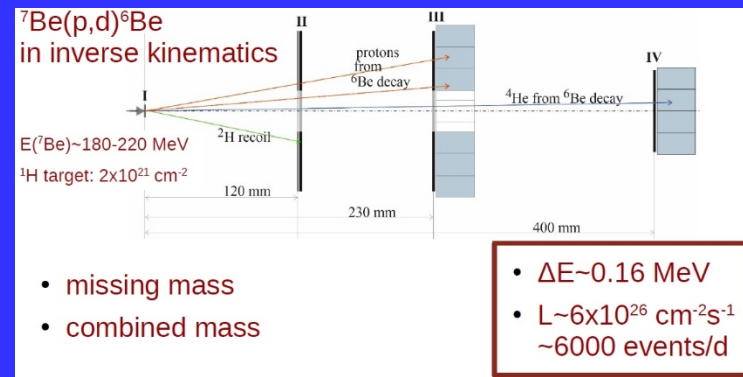
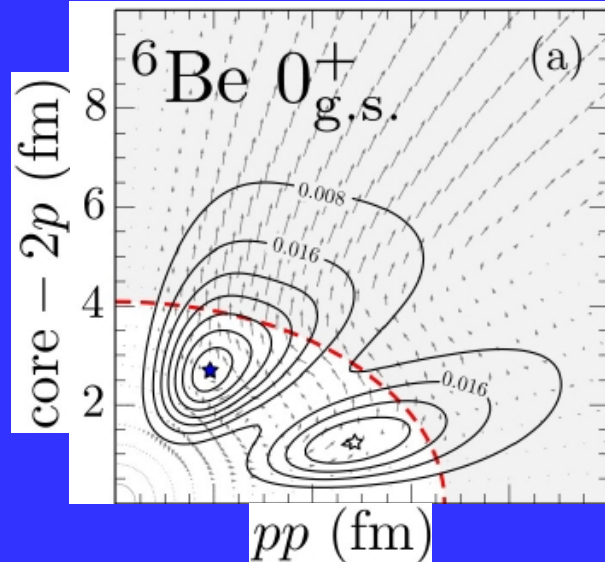
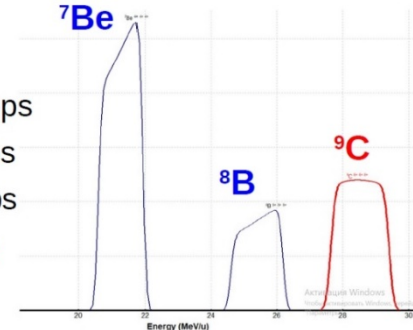
Light proton-rich nuclei ${}^6\text{Be}$, ${}^7\text{B}$, ${}^8\text{C}$ studied by the (p,d) reaction

${}^6\text{Be}$ states	E_T (MeV)	Γ (MeV)	
0_1^+	1.383 (1.370)	0.041 (0.092)	
0_2^+	5.95	11.21	
1^+	4.76	7.75	<i>Exp.</i>
2_1^+	2.90 (3.04)	1.05 (1.16)	
2_2^+	4.63	5.67	

Myo and K. Kato, Phys. Rev. C **107** (2023) 014301.

Tuning ACCULINNA-2 for ${}^7\text{Be}$, ${}^8\text{B}$, ${}^9\text{C}$ beams

- primary beam of ${}^{12}\text{C}$, 50 MeV/A, 2 μA :
 - ${}^7\text{Be}$, ~ 27 MeV/A, 1.1×10^5 pps
 - ${}^8\text{B}$, ~ 32 MeV/A, 4.4×10^4 pps
 - ${}^9\text{C}$, ~ 36 MeV/A, 6.8×10^4 pps
- All component available in one beam mixture

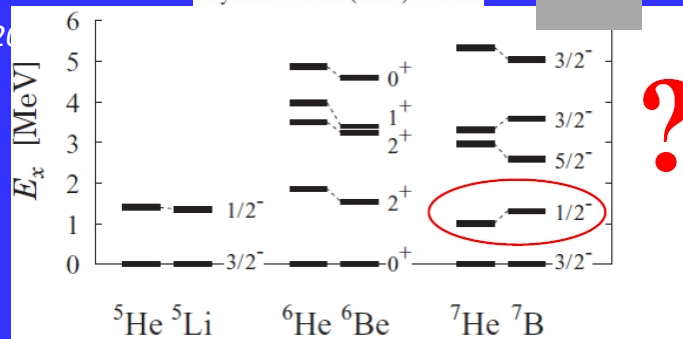


- missing mass
- combined mass

- $\Delta E \sim 0.16$ MeV
- $L \sim 6 \times 10^{26} \text{ cm}^{-2}\text{s}^{-1}$
- ~ 6000 events/d

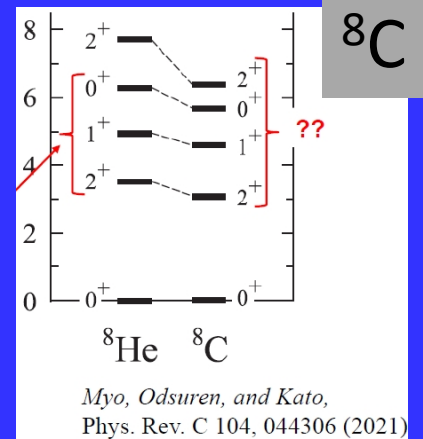
S. M. Wang et al., PRC 99, 054302 (2019)

T. Myo, Y. Kikichi and K. Kato, Phys. Rev. C **84** (2011) 064306



${}^7\text{B}$

?



${}^8\text{C}$

Myo, Odsuren, and Kato, Phys. Rev. C **104**, 044306 (2021)

Summary

1. Effective methods for the study of light exotic nuclear systems near and beyond nucleon drip-line were developed in experiments at the ACCULINNA fragment separator, JINR FLNR. New important results on the structure and level scheme of exotic nuclei as ${}^6\text{He}$, ${}^5\text{H}$, ${}^9\text{He}$, ${}^{10}\text{He}$ were obtained. These techniques are based on intense radioactive beams (${}^6\text{He}$, ${}^8\text{He}$, ${}^3\text{H}$), unique targets (including tritium) and correlation methods especially efficient for direct reactions studies at intermediate energies.
2. In two experiments at newly commissioned fragment separator ACCULINNA-2 a solid experimental evidence for two resonant states of ${}^7\text{H}$ are located at 2.2(5) and 5.5(3) MeV relative to the ${}^3\text{H}+4\text{n}$ decay threshold is provided. There are indications that the resonant states at 7.5(3) and 11.0(3) MeV. Based on the energy and angular distributions, obtained for the studied ${}^2\text{H}({}^8\text{He}, {}^3\text{He}){}^7\text{H}$ reaction, the weakly populated 2.2(5)-MeV peak is ascribed to the ${}^7\text{H}$ ground state. It is highly plausible that the 5.5(3)-MeV state is the $5/2^+$ member of the ${}^7\text{H}$ excitation of $5/2^+ - 3/2^+$ doublet, built on the 2^+ configuration of valence neutrons. The supposed 7.5-MeV state can be another member of this doublet
3. The ${}^6\text{H}$ spectrum was populated in the ${}^2\text{H}({}^8\text{He}, {}^4\text{He}){}^6\text{H}$ transfer reaction. The broad bump in the ${}^6\text{H}$ MM spectrum at $E = 6.8(5)$ MeV with $\Gamma \sim 5.5$ MeV is reliably identified with the population cross section $d\sigma/d\Omega_{\text{CM}} = 190 \mu\text{b/sr}$ in the $5^\circ < \Theta_{\text{CM}} < 16^\circ$ angular range.
4. *No evidence* for the $\approx 2.6\text{--}2.9$ MeV state in ${}^6\text{H}$ was found, which was reported in 3 previous works. The cross section limit $d\sigma/d\Omega_{\text{CM}} \leq 5 \mu\text{b/sr}$ is set for the population of possible states with $E < 3.5$ MeV. We suggest that the position of the ${}^6\text{H}$ g.s. is not yet established and discussion of this issue should be continued.
5. After U400M cyclotron modernization, the future planes of the possible experiments are discussed. Most likely that could be study of ${}^8\text{He}+{}^4\text{He}$ scattering, the detailed spectroscopy of ${}^5\text{H}$ - ${}^5\text{He}$, the further research of ${}^6\text{Be}$ nucleus and search for isobar-analogue states in proton-rich nuclei ${}^7\text{B}$ and ${}^8\text{C}$.

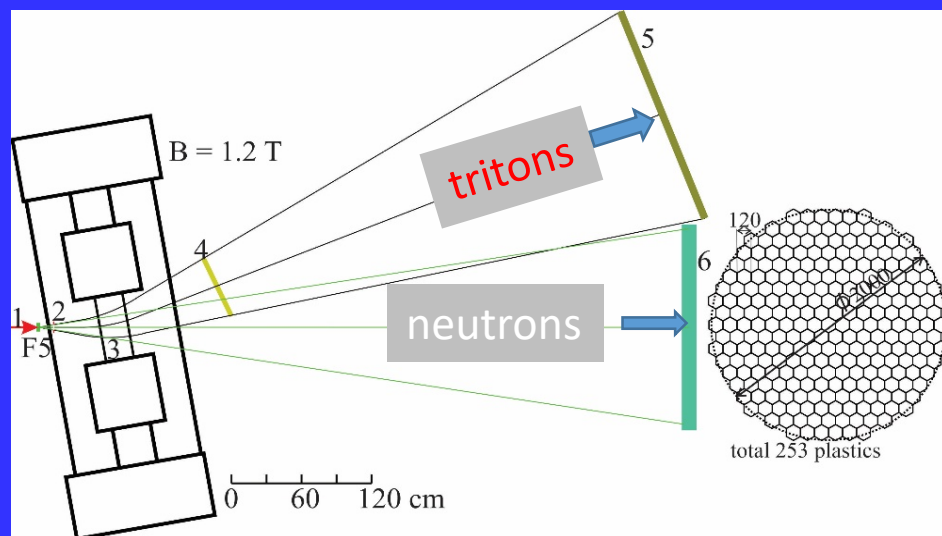
A. S. Fomichev, I. A. Muzalevskii , A. A. Bezbakh, E. Yu. Nikolskii, V. Chudoba, S. A. Krupko, S. G. Belogurov, D. Biare,
E. M. Gazeeva, M.S. Golovkov, A. V. Gorshkov, L. V. Grigorenko, G. Kaminski, , D. A. Kostyleva,
M. Yu. Kozlov, B. Mauyey, Yu. L. Parfenova, W. Piatek, A. M. Quynh, V. N. Schetinin, A. Serikov,
S. I. Sidorchuk, P. G. Sharov, R. S. Slepnev, S. V. Stepanov, A. Swiercz, P. Szymkiewicz,
G. M. Ter-Akopian, R. Wolski, B. Zalewski

ACCULINNA-2 team



Thank you for your attention!

1. Tritium Target !! Liquid $T_2 \sim 3 \cdot 10^{21} \text{ cm}^{-2}$



Ground-state energy resolution $\sim 400 \text{ keV}$

Liquid $T_2 \sim 3 \cdot 10^{21} \text{ cm}^{-2}$

Intensity of ${}^8\text{He} \sim 10^5 \text{ 1/s}$

Reaction cross section $\sim 0.1 \text{ mb/sr}$

Triton trigger eff. ~ 0.7

$t+4n$ detection eff. ~ 0.015

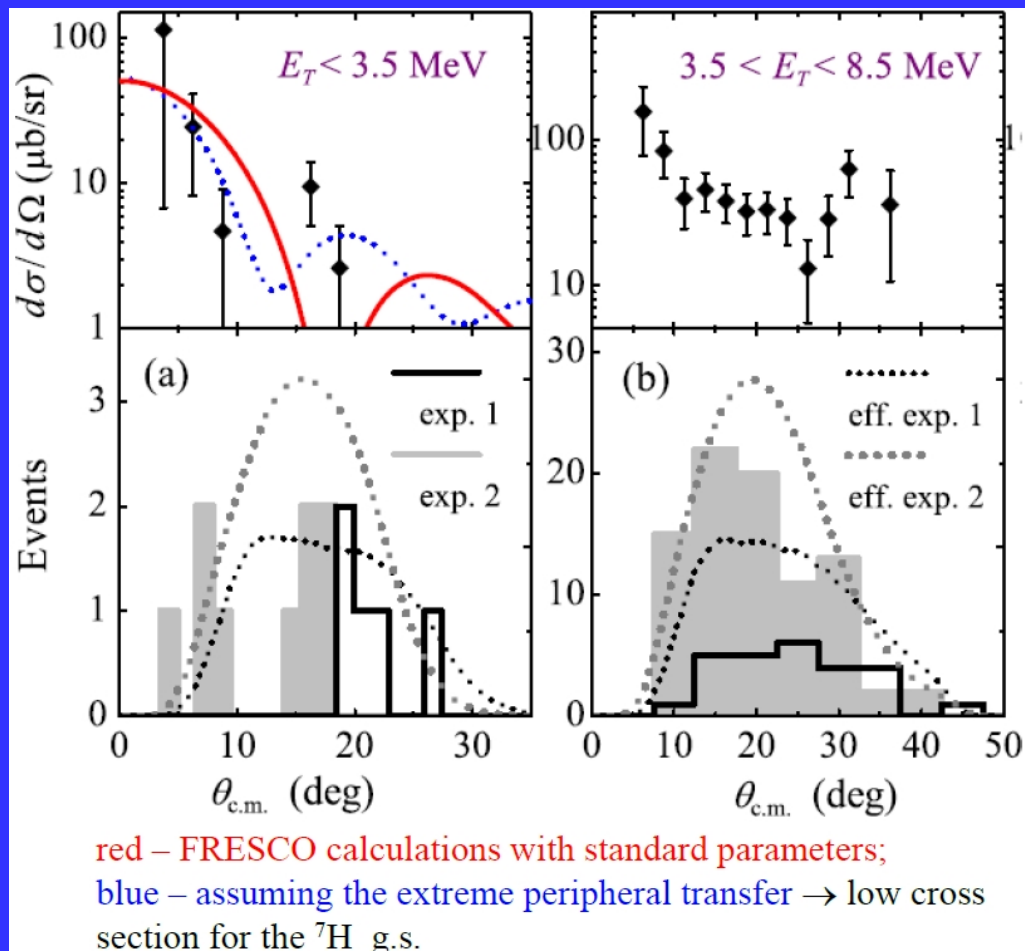
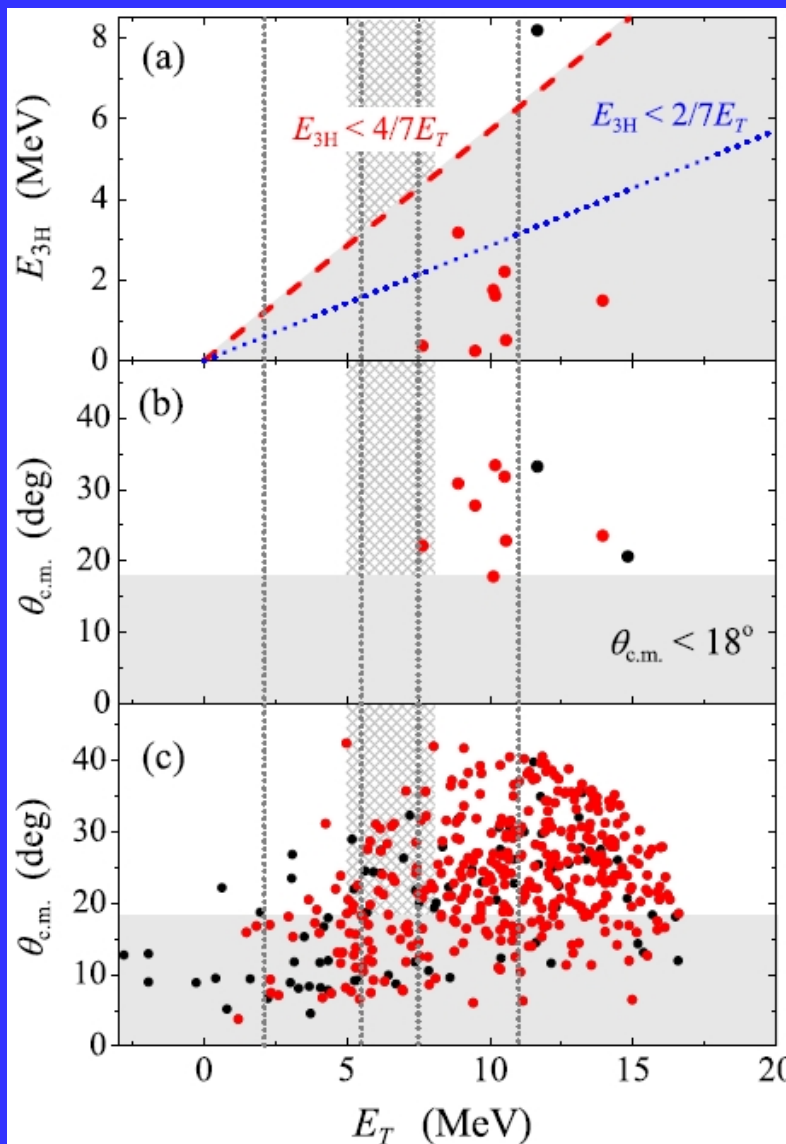
${}^7\text{H}_{\text{g.s.}}$ counting rate: $\sim 5 \text{ per day}$

2. $p({}^{11}\text{Li}, p{}^4\text{He}){}^7\text{H}$ ${}^{11}\text{Li}$ – new “source” to make ${}^7\text{H}$

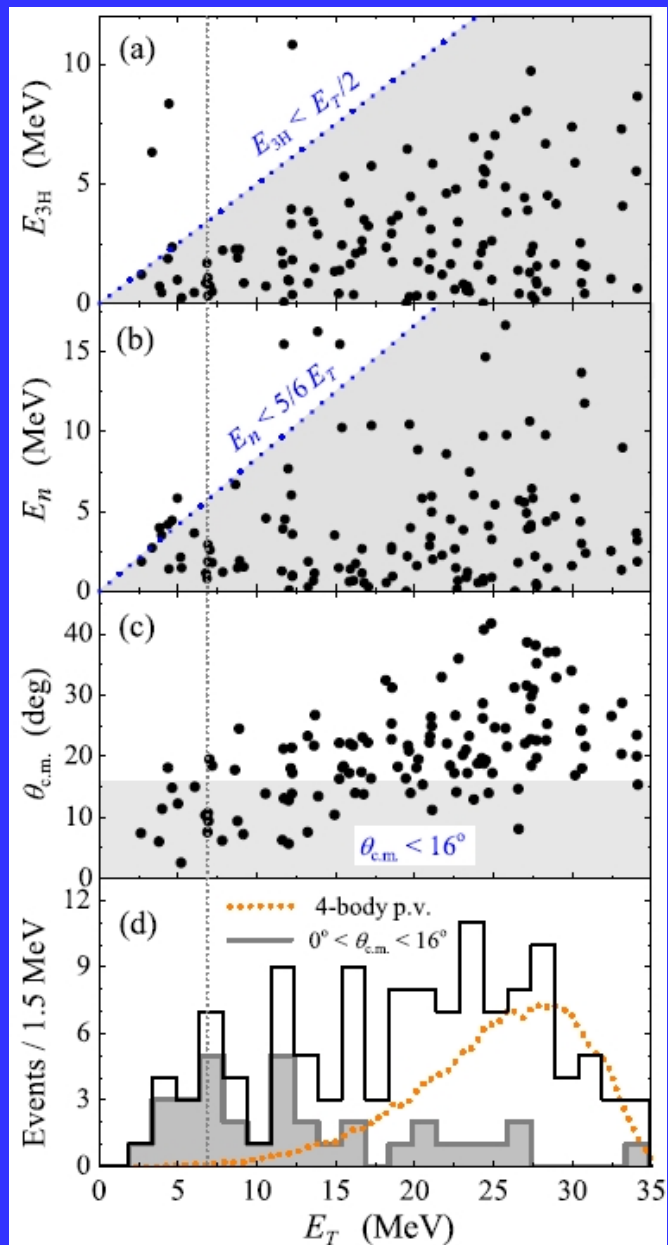
Quasi-free alpha knockout from ${}^{11}\text{Li}$ possibly has larger cross section
 ${}^7\text{H}$ could have $[s^2p^2]$ component of WF that already exist in ${}^{11}\text{Li}$

The c.m. angular distributions for the $2\text{H}(8\text{He}, 3\text{He})7\text{H}$ reaction in different 7H MM energy ranges

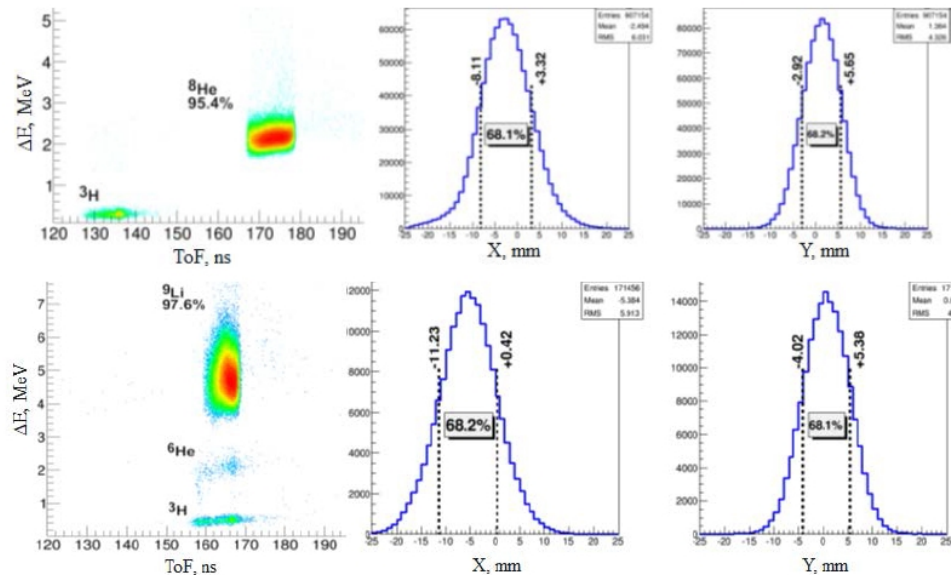
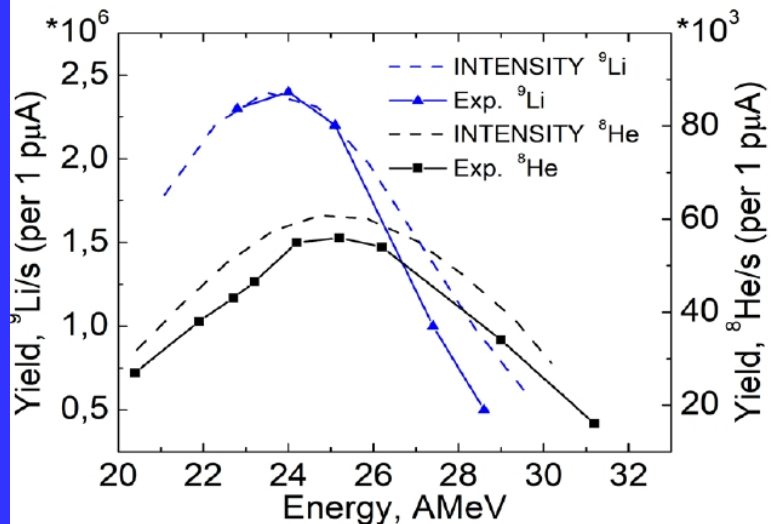
Empty target from the 2nd Run



4He+t+n coincidences



Characteristics of several RIBs at ACCULINNA-2 obtained in the first experiments



The observed basic characteristics for RIBs (intensity, purity, beam profiles in final focal plane) are in a good agreement with the technical specification and estimations.

Ion	E, AMeV	Reaction	I, pps/pμA	P, %	X_Y, mm (FWHM)	Δp, ±%	Wedge Be, mm
⁶ He	29	¹¹ B(33.5 AMeV)+Be(1 mm)	2.2*10 ⁶	90.2	10_8	2.0	1.0
⁸ He	28	--"	5.5*10 ⁴	95.4	9_7	3.25	1.0
⁹ Li	31	--"	5.0*10 ⁵	97.6	12_9	2.0	1.0
¹⁰ Be	45	¹⁵ N (49.3 AMeV)+Be(1 mm)	2.3*10 ⁶	78.4	16_11	1.25	1.0
²⁶ P	28	³² S (52.7 AMeV)+Be (0.5 mm)	15	<0.5	18_12	0.75	0.5
²⁷ S	27	--"	60	1	18_12	0.75	0.5

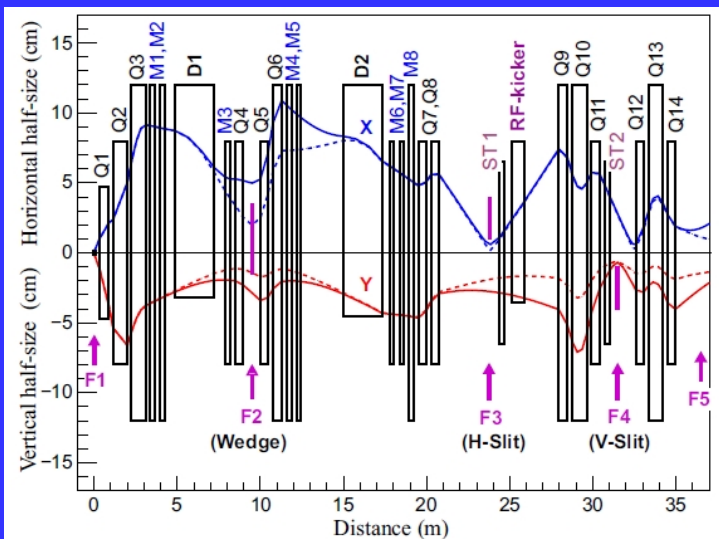


Fig. 4. Envelopes of the beam in horizontal (X) and vertical (Y) planes. F1 object slit is $2 \times 2 \text{ mm}^2$, capture angles are ± 30 and $\pm 35 \text{ mrad}$ in X and Y planes, respectively. Solid lines are for $\delta_P = \pm 2.5\%$ and dashed ones for $\delta_P = \pm 1.0\%$.

Table 4. Ion-optical parameters of ACCULINNA-2 magnetic dipoles $D1$, $D2$ and steering (correcting) magnets $ST1$, $ST2$.

Value	Units	$D1$	$D2$	$ST1, ST2$	
Bending direction		horizontal	horizontal	vertical	
Type		sector	sector	rectangular	
Gap height	$2h$	cm	6.4	9.0	11.2
Bending mean radius	R	m	3.0	3.0	-
Bending field	B_{nom}	T	1.3	1.3	0.053
Length	L_{eff}	m	2.356	2.356	0.283
Working width	$2w$	cm	20	20	10
Bending angle	Φ	dgr	45	45	-
Entrance angle	τ_{entr}	dgr	0	0	0
Exit angle	τ_{exit}	dgr	0	20	0

Table 5. Ion-optical parameters of ACCULINNA-2 magnetic quadrupoles.

Value	units	$Q1$	$Q2$	$Q3, 10, 13$	$Q4, 5, 7, 8, 11, 12, 14$	$Q6, 9$	
Aperture	$2r$	cm	9.4	16	24	16	24
Length	L_{eff}	cm	54.3	87.1	85.9	47.6	51.8
Field gradient	G_{nom}	T/m	9.2	7.2	7.2	9.8	6.4

Table 6. Ion-optical parameters of magnetic multipoles. They all have an effective length $L_{eff} = 28.6 \text{ cm}$.

Multipole	Aperture	Sextupole	Octupole
	$2r$, cm	B''_{nom} , T/m ²	B'''_{nom} , T/m ³
$M1, M2, M4, M5, M8$	24	3.9	195
$M3, M6, M7$	16	39	

Table 3. Main ion-optical parameters of ACCULINNA-2.

Primary beam spot size	F1	2×2	mm^2
Momentum acceptance		6.0	%
θ_{0x} angular acceptance		60	mrad
θ_{0y} angular acceptance		70	mrad
X momentum dispersion	F1 \rightarrow F2	2.0	$\text{cm}/\%B\rho$
θ_x angl. mom. disper.	-	0.5	$\text{mrad}/\%B\rho$
X magnification	-	-1.0	
Y magnification	-	-7.4	
X momentum dispersion	F2 \rightarrow F3	3.3	$\text{cm}/\%B\rho$
X magnification	-	-1.7	
Y magnification	-	-2.0	
X magnification	F1 \rightarrow F3	1.7	
Y magnification	-	5.0	
Length	F1 \rightarrow F2	9.51	m
Length	F2 \rightarrow F3	14.35	m
Length	F3 \rightarrow F4	7.63	m
Length	F3 \rightarrow F5	13.25	m
Length	F1 \rightarrow F5	37.1	m

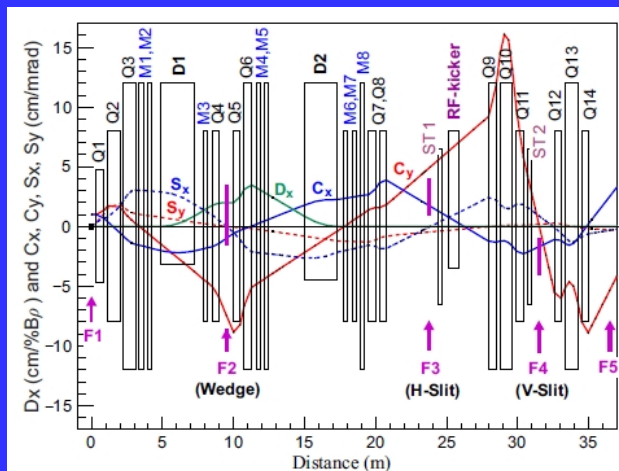


Fig. 6. Momentum dispersion $D_x = (x/\delta_P)$ and main first-order cosine-like, $C_x = (x/x_0)$, $C_y = (y/y_0)$ and sine-like $S_x = (x/\theta_{0x})$, $S_y = (y/\theta_{0y})$ trajectories.

Ion	E, AMeV	Reaction	I, pps/pμA	P, %	X_Y, mm (FWHM)	Δp, ±%	Wedge Be, mm
⁶ He	29	¹¹ B(33.5 AMeV)+Be(1 mm)	2.2*10 ⁶	90.2	10_8	2.0	1.0
⁸ He	28	--"--	5.5*10 ⁴	95.4	9_7	3.25	1.0
⁹ Li	31	--"--	5.0*10 ⁵	97.6	12_9	2.0	1.0
¹⁰ Be	45	¹⁵ N (49.3 AMeV)+Be(1 mm)	2.3*10 ⁶	78.4	16_11	1.25	1.0
²⁶ p	28	³² S (52.7 AMeV)+Be (0.5 mm)	15	<0.5	18_12	0.75	0.5
²⁷ S	27	--"--	60	1	18_12	0.75	0.5

The ID plot for neutron spectrometer

